British Journal of Pharmacology

DOI:10.1111/j.1476-5381.2010.01169.x
www.brjpharmacol.org

RESEARCH PAPER

Ca^{2+} entry following P2X receptor activation induces IP_3 receptor-mediated Ca^{2+} release in myocytes from small renal arteries

Oleksandr V Povstyan[1,2], Maksym I Harhun[1] and Dmitri V Gordienko[1,2]

[1]*Division of Basic Medical Sciences, St. George's, University of London, London, UK, and* [2]*Laboratory of Molecular Pharmacology and Biophysics of Cell Signalling, Bogomoletz Institute of Physiology, Kyiv, Ukraine*

Correspondence
Dr Dmitri Gordienko, Ion Channels and Cell Signalling Centre, Division of Basic Medical Sciences, St. George's, University of London, Cranmer Terrace, London SW17 0RE, UK. E-mail: gordienk@sgul.ac.uk

Keywords
renal vascular smooth muscle cells; $\alpha\beta$-meATP; NF 279; MRS 2578; Ca^{2+} signalling; P2X receptor; voltage-gated Ca^{2+} channels; inositol 1,4,5-trisphosphate receptor; ryanodine receptor; sarcoplasmic reticulum

Received
30 March 2010
Revised
4 November 2010
Accepted
25 November 2010

BACKGROUND AND PURPOSE

P2X receptors mediate sympathetic control and autoregulation of the renal circulation triggering contraction of renal vascular smooth muscle cells (RVSMCs) via an elevation of intracellular Ca^{2+} concentration ($[Ca^{2+}]_i$). Although it is well-appreciated that the myocyte Ca^{2+} signalling system is composed of microdomains, little is known about the structure of the $[Ca^{2+}]_i$ responses induced by P2X receptor stimulation in vascular myocytes.

EXPERIMENTAL APPROACHES

Using confocal microscopy, perforated-patch electrical recordings, immuno-/organelle-specific staining, flash photolysis and RT-PCR analysis we explored, at the subcellular level, the Ca^{2+} signalling system engaged in RVSMCs on stimulation of P2X receptors with the selective agonist $\alpha\beta$-methylene ATP ($\alpha\beta$-meATP).

KEY RESULTS

RT-PCR analysis of single RVSMCs showed the presence of genes encoding inositol 1,4,5-trisphosphate receptor type 1(IP_3R1) and ryanodine receptor type 2 (RyR2). The amplitude of the $[Ca^{2+}]_i$ transients depended on $\alpha\beta$-meATP concentration. Depolarization induced by 10 $\mu mol \cdot L^{-1}$ $\alpha\beta$-meATP triggered an abrupt Ca^{2+} release from sub-plasmalemmal ('junctional') sarcoplasmic reticulum enriched with IP_3Rs but poor in RyRs. Depletion of calcium stores, block of voltage-gated Ca^{2+} channels (VGCCs) or IP_3Rs suppressed the sub-plasmalemmal $[Ca^{2+}]_i$ upstroke significantly more than block of RyRs. The effect of calcium store depletion or IP_3R inhibition on the sub-plasmalemmal $[Ca^{2+}]_i$ upstroke was attenuated following block of VGCCs.

CONCLUSIONS AND IMPLICATIONS

Depolarization of RVSMCs following P2X receptor activation induces IP_3R-mediated Ca^{2+} release from sub-plasmalemmal ('junctional') sarcoplasmic reticulum, which is activated mainly by Ca^{2+} influx through VGCCs. This mechanism provides convergence of signalling pathways engaged in electromechanical and pharmacomechanical coupling in renal vascular myocytes.

Abbreviations

2-APB, 2-aminoethoxydiphenyl borate; $\alpha\beta$-meATP, $\alpha\beta$-methylene ATP; CICR, Ca^{2+}-induced Ca^{2+} release; CPA, cyclopiazonic acid; IP_3, inositol 1,4,5-trisphosphate; IP_3R, inositol 1,4,5-trisphosphate receptor; jSR, sub-plasmalemmal ('junctional') sarcoplasmic reticulum; MRS2578, N,N''-1,4-butanediylbis[N'-(3-isothiocyanatophenyl)thio urea; NF279, 8,8'-[carbonylbis(imino-4,1-phenylenecarbonylimino-4,1-phenylenecarbonyl-imino)] bis(1,3,5-naphthalene-trisulphonic acid); PLC, phospholipase C; RBF, renal blood flow; RSNA, renal sympathetic nerve activity; RT-PCR, reverse transcription polymerase chain reaction; RVSMC, renal vascular smooth muscle cells; RyR, ryanodine receptor; SERCA, sarco-/endoplasmic reticulum Ca^{2+}-ATPase; SPCU, sub-plasmalemmal $[Ca^{2+}]_i$ upstroke; SR, sarcoplasmic reticulum; U-73122, 1-[6-([(17β)-3-methoxyestra-1,3,5(10)-trien-17-yl]amino)hexyl]-1H-pyrrole-2,5-dione; U-73343, 1-[6-([(17β)-3-methoxyestra-1,3,5(10)-trien-17-yl]amino)hexyl]-2,5-pyrrolidinedione; edelfosine (7R)-4-hydroxy-7-methoxy-N,N,N-trimethyl-3,5,9-trioxa-4 -phosphaheptacosan-1-aminium-4-oxide; VGCC, voltage-gated Ca^{2+} channel

Introduction

Renal blood flow (RBF) accounts for 20–25% of cardiac output at rest (Malpas and Leonard, 2000; Cupples and Braam, 2007). The mechanisms controlling contraction/relaxation of renal vascular smooth muscle cells (RVSMCs), which regulate the diameter of renal resistance arteries and hence RBF and glomerular filtration rate, play a fundamental role in the control of systemic blood pressure (DiBona, 2004; Navar, 2005).

Vascular myocytes are stimulated to contract by elevation of intracellular Ca^{2+} concentration ($[Ca^{2+}]_i$) resulting in activation of Ca^{2+}/calmodulin-dependent myosin light chain kinase which causes force development via myosin light chain phosphorylation (Walsh, 1994). An increase in $[Ca^{2+}]_i$ in smooth muscle cell (SMC) is caused by either depolarization of the myocyte membrane (electromechanical coupling; Somlyo and Somlyo, 1968) resulting from activation of ionotropic receptors or metabotropic receptor-coupled cationic channels and leading to Ca^{2+} influx via voltage-gated Ca^{2+} channels (VGCCs), or by activation of metabotropic receptors (pharmacomechanical coupling; Somlyo and Somlyo, 1968) coupled via $G_{q/11}$-protein to phospholipase C (PLC) activation followed by inositol 1,4,5-trisphosphate (IP_3) liberation and IP_3 receptor (IP_3R)-mediated Ca^{2+} release, or by a combination of these mechanisms (Bolton *et al.*, 1999; Davis and Hill, 1999; Wray and Burdyga, 2010). Either of these events, which cause an initial rise in $[Ca^{2+}]_i$, may be further augmented by ryanodine receptor (RyR)-mediated Ca^{2+} release activated via a Ca^{2+}-induced Ca^{2+} release (CICR) mechanism (Fabiato and Fabiato, 1975). However, the recruitment of RyR-mediated Ca^{2+} release by voltage-gated Ca^{2+} entry and/or IP_3R-mediated Ca^{2+} release in smooth muscles is still an area of extensive debate and controversy (reviewed in Laporte *et al.*, 2004; Wray and Burdyga, 2010). Indeed, the relative contribution of RyRs and IP_3Rs to intracellular $[Ca^{2+}]_i$ mobilization varies in different types of SMCs, and often depends on the strengths and mechanism of SMC stimulation. In some phasic smooth muscles, for example, urinary bladder and vas deferens, Ca^{2+} entry through VGCCs is tightly coupled to RyR-mediated Ca^{2+} release. Electrical stimulation of these SMCs, in which close proximity of VGCCs and RyRs within the caveolar domains was confirmed with 3D-immunofluorescence and electron microscopy (Moore *et al.*, 2004), triggers an abrupt RyR-mediated Ca^{2+} release at multiple sub-PM regions ('hot spots', Ohi *et al.*, 2001; Morimura *et al.*, 2006). The ability of Ca^{2+} entering the SMC via VGCCs to induce RyR-mediated Ca^{2+} release has also been demonstrated in voltage-clamp experiments performed on SMCs from pregnant myometrium (Shmigol *et al.*, 1998), ileum (Kohda *et al.*, 1997), mesenteric artery (Bolton and Gordienko, 1998), cerebral arteries (Kamishima and McCarron, 1997) and portal vein (Coussin *et al.*, 2000). However, other research groups working on different or even the same SMC type failed to detect any evidence of CICR (Fleischmann *et al.*, 1996; Kamishima and McCarron, 1996; Bradley *et al.*, 2002). The ability of Ca^{2+} liberated via IP_3Rs to trigger RyR-mediated Ca^{2+} release also varies among different types of smooth muscles and depends on receptor distribution and isoform expression (reviewed in Wray and Burdyga, 2010). Emerging evidence highlights the importance of RyRs and CICR in calcium signalling and arteriolar contraction in the renal microcirculation. It was demonstrated that in these arterioles RyR/CICR contribute to $[Ca^{2+}]_i$ responses initiated by Ca^{2+} entry and by IP_3R-mediated Ca^{2+} release (reviewed in Arendshorst and Thai, 2009).

Two major sympathetic cotransmitters, noradrenaline and ATP, mediate vasoconstriction of small arteries (Wier *et al.*, 2009) by acting on metabotropic α_1-adrenoceptors and ionotropic P2X receptors respectively. Thus, P2X receptors provide an important therapeutic target, mediating substantial vasoconstrictor drive resistant to adrenoceptor antagonists (Wier *et al.*, 2009).

In the kidney, apart from sympathetic transmission, ATP is involved in paracrine regulation. On being released by apical macula densa cells in response to an increase in NaCl concentration in the distal tubular fluid (Bell *et al.*, 2003), ATP triggers P2X receptor-mediated vasoconstriction of afferent arterioles (Inscho *et al.*, 2003), thus decreasing RBF and glomerular filtration rate. This tubuloglomerular feedback mechanism (Nishiyama *et al.*, 2000; Guan *et al.*, 2007a; Surprenant and North, 2009) and myogenic mechanism are two important components of renal autoregulation (Cupples and Braam, 2007).

The respective role of RyRs and IP_3Rs in smooth muscle contraction is an area of active investigation. Although RyRs and IP_3Rs are both Ca^{2+}-sensitive and can activate each other via CICR mechanism, leading to an all-or-none regenerative response, graded Ca^{2+} signals have been reported to be evoked by increasing stimuli targeting RyRs (Isenberg and Han, 1994) or IP_3Rs (Bootman *et al.*, 1994). The resolution of this paradox has been suggested to lie in the local control of Ca^{2+} microdomains that function and are regulated autonomously (Berridge, 1997), the gradual recruitment of which by gradually increasing stimuli would result in graded Ca^{2+} signals. Imaging microdomain Ca^{2+} in muscle cells has reshaped our understanding of Ca^{2+} signalling and provided direct evidence to validate the local control theory in skeletal, cardiac and smooth muscles (Wang *et al.*, 2004; McCarron *et al.*, 2006).

In smooth muscles, IP_3R-mediated Ca^{2+} release is essential for $[Ca^{2+}]_i$ mobilization and contraction, especially (but not exclusively) induced by stimulation with neurotransmitters and hormones (Boittin *et al.*, 1999; Bayguinov *et al.*, 2000; McCarron *et al.*, 2002; Zhang *et al.*, 2003; Lamont and Wier, 2004; MacMillan *et al.*, 2005; Gordienko *et al.*, 2008). The role of IP_3Rs seems to be to facilitate CICR within and between RyRs domains (Boittin *et al.*, 1998; Gordienko and Bolton, 2002; White and McGeown, 2002; Zhang *et al.*, 2003). However, a cooperative relationship between IP_3Rs and RyRs is not always the rule. When both receptor types share the same calcium store, the interplay between them can be regulated via alterations in the sarcoplasmic reticulum (SR) calcium load. For example, in SMCs from both the gastric antrum and vas deferens block of IP_3Rs, which caused an elevation of the caffeine-releasable store content, increased spontaneous Ca^{2+} spark activity (White and McGeown, 2002, 2003).

Another important aspect of the SMC Ca^{2+} signalling system is the regulation of IP_3R-mediated Ca^{2+} release by $[Ca^{2+}]_i$. In vascular SMCs of small arteries, Lamont and Wier (2004) concluded that if RyRs were blocked, cell-wide Ca^{2+} waves could still be evoked by strong activation of

adrenoceptors leading to myocyte and vessel contraction. Thus, CICR apparently can occur among IP_3Rs alone, although normally, at low levels of adrenoceptor activation RyRs are needed to trigger IP_3R dependent Ca^{2+} waves (Wier and Morgan, 2003). Furthermore, activation of IP_3Rs by a localized increase in $[Ca^{2+}]_i$ was directly demonstrated in an elegant experiment conducted on rabbit urinary bladder myocytes; IP_3R-mediated Ca^{2+} release was found to be induced by local Ca^{2+} uncaging (Ji *et al.*, 2006).

We have previously demonstrated that following activation of muscarinic receptors in intestinal myocytes IP_3R-mediated Ca^{2+} release is facilitated by Ca^{2+} influx via VGCCs (Gordienko *et al.*, 2008). Although M_3 receptors are linked to a $G_{q/11}/PLC/IP_3/Ca^{2+}$ signalling pathway, we hypothesized that in contrast to cardiac muscle, excitation–contraction (E–C) coupling in smooth muscle occurs by Ca^{2+} entry through VGCCs, which evokes IP_3R-mediated Ca^{2+} release via CICR mechanism. This hypothesis needs to be tested in vascular myocytes regulated by ionotropic receptors, which are not coupled to the $G_{q/11}$-GTP/PLC/IP_3 system.

Taking into account the importance of ionotropic P2X receptors (Burnstock, 2007; Surprenant and North, 2009) in the regulation of renal circulation (Malpas and Leonard, 2000; Inscho *et al.*, 2003; Cupples and Braam, 2007; Guan *et al.*, 2007a), we tested our hypothesis on RVSMCs, which, as we have recently demonstrated, express functional monomeric P2X1 and heteromeric P2X1/4 receptors (Harhun *et al.*, 2010). We found that depolarization of RVSMCs following P2X receptor activation induces IP_3R-mediated Ca^{2+} release from sub-plasmalemmal ('junctional') sarcoplasmic reticulum (jSR), which is activated mainly by Ca^{2+} influx through VGCCs. Our results support the notion that, in contrast to cardiac muscle, E–C coupling in vascular smooth muscle may occur by Ca^{2+} entry through VGCCs, which evokes an initial IP_3R-mediated Ca^{2+} release activated via a CICR mechanism. A preliminary account of this study has been published in abstract form (Povstyan *et al.*, 2009).

Methods

Isolation of renal vascular smooth muscle cells (RVSMCs)

Male Wistar Kyoto rats (180–250 g, 65 animals obtained from Charles Rivers laboratories) were humanely killed by decapitation after cervical dislocation as approved under Schedule 1 of the UK Animals (Scientific Procedures) Act 1986. Interlobar and arcuate arteries were dissected from the kidney as described previously (Gordienko *et al.*, 1994). Following the dissection, the blood vessels with outer diameter of 50–150 μm were cut into 1–2 mm pieces and collected in ice-cold physiological salt solution (PSS) containing (in $mmol \cdot L^{-1}$): NaCl 120, KCl 6, $CaCl_2$ 2.5, $MgCl_2$ 1.2, glucose 12, HEPES 10; pH adjusted to 7.4 with NaOH. After a 10 min rinse in Ca^{2+}-free PSS, the tissue samples were transferred into the same solution supplemented with ($mg \cdot mL^{-1}$): protease (Type X) 0.75, collagenase (Type 1A) 1.5, soybean trypsin inhibitor 1 and bovine serum albumin 1, and incubated for 20 min at 37 °C. The tissue samples were then rinsed for 10 min in an enzyme-free Ca^{2+}-free solution and triturated using a glass Pasteur pipette. Isolated RVSMCs were obtained by several cycles of trituration, each followed by transfer to fresh solution with gradually increasing $[Ca^{2+}]$ (from 0.125 to 1.25 $mmol \cdot L^{-1}$). Transfer of the tissue samples to fresh solution before trituration facilitated removal of debris and damaged cells from the suspension, while gradually increasing $[Ca^{2+}]$ in the medium prevented the myocytes from 'calcium shock' and hypercontraction (Gordienko and Zholos, 2004). Small aliquots of the cell suspension were transferred to the experimental chambers and diluted with PSS. RVSMCs were then either collected for reverse transcription polymerase chain reaction (RT-PCR) experiments or used for electrical recording and confocal imaging within 8 h of isolation.

RNA isolation and RT-PCR analysis

Reverse transcription polymerase chain reaction analysis was performed using single isolated RVSMCs. The myocytes (pool of ~500 cells per sample) were collected under a microscope using a wide-bore glass micropipette and frozen immediately after collection. Total RNA was extracted using the Qiagen RNeasy extraction kit (Qiagen, Crawley, UK). cDNA was obtained using Superscript II Reverse Transcriptase (Invitrogen, Paisley, UK) and used in RT-PCR. cDNA was used as a template in a 50 μL RT-PCR reaction containing 1.5 $mmol \cdot L^{-1}$ $MgCl_2$, 0.2 $mmol \cdot L^{-1}$ deoxynucleoside triphosphates, 0.2 $\mu mol \cdot L^{-1}$ forward and reverse primers (Invitrogen), and 2.5 units of platinum *Taq* DNA polymerase (Invitrogen). Amplification was performed using a Touchgene Thermocycler (Bibby Scientific Ltd., Staffordshire, UK) according to the following schedule: 94°C for 2 min; 40 cycles (for brain and liver tissue preparations) or 45 cycles (for RVSMC samples) of 94°C for 30 s; 57°C for 60 s; and 72°C for 3 min, followed by a final elongation period of 10 min at 72°C. No-template control PCR was also performed simultaneously with every reaction. To avoid detecting genomic DNA contamination, primers were designed to span at least one intron of the genomic sequence for genes encoding proteins of interest. The experiments were repeated with at least four samples of RVSMCs obtained from different animals. The purity of the RVSMC sample was confirmed by the expression of the gene encoding the SMC marker, smooth muscle myosin heavy chain, but not the markers for other types of cell present in the vascular wall such as: fibroblasts and endothelial cells (CD34), neurones (PGP9.5) and pericytes (NG2), as previously described (Harhun *et al.*, 2009; 2010). PCR products were separated and visualized in ethidium bromide-stained 2% agarose gel by electrophoresis.

The following primers (the data in parentheses show: Genebank accession number, the sense bordering nucleotide position, the anti-sense bordering nucleotide position) were used in this study: β-actin (NM_031144, 306–325, 1007–1026), smooth muscle myosin heavy chain for SMCs (X16262, 447–466, 1182–1191), CD34 for endothelial cells and fibroblasts (NM_001107202, 50–69, 882–901), PGP9.5 for neurones (D10699, 54–73, 544–563), NG2 proteoglycan for pericytes (NM_031022, 1815–1834, 2791–2810), inositol 1,4,5-trisphosphate (IP_3) receptor type 1 (NM_001007235, 6244–6263, 7030–7049), IP_3 receptor type 3 (NM_013138, 6142–6161, 7088–7107), ryanodine receptor type 1 (XM_001078539, 8038–8057, 8811–8830), ryanodine

receptor type 2 (NM_032078, 8513–8532, 9317–9336), ryanodine receptor type 3 (XM_342491, 8035–8054, 9101–9120).

Drug application

Renal vascular smooth muscle cells were stimulated with $\alpha\beta$-methylene ATP ($\alpha\beta$-meATP) and caffeine which were applied as a 2 s pulse through a glass micropipette attached to the outlet of a pressure ejector Picospritzer III (Intracel Ltd, Royston, Hertfordshire, UK). Similar application of the control solution (without agonist) had no effect on $[Ca^{2+}]_i$. In the experiments where the same RVSMC was stimulated with $\alpha\beta$-meATP and caffeine or different concentrations of $\alpha\beta$-meATP, the agonist-containing micropipette was replaced in between successive agonist applications. Antagonists were superfused through the experimental bath.

Visualization of $[Ca^{2+}]_i$ changes

Changes of $[Ca^{2+}]_i$ in isolated RVSMCs were imaged using the high-affinity fluorescent Ca^{2+} indicators Fluo-4 or Fluo-3. Fluo-4 was loaded by incubating the RVSMCs for 20 min with 5 $\mu mol \cdot L^{-1}$ fluo-4 acetoxymethyl ester (Fluo-4 AM; diluted from a stock containing 2 $mmol \cdot L^{-1}$ Fluo-4 AM and 0.025% ($w \cdot v^{-1}$) pluronic F-127 in dimethyl sulphoxide) followed by a 40 min wash in PSS to allow time for de-esterification. Fluo-3 was loaded through the patch pipette by dialysis of the myocyte with a solution containing 0.1 $mmol \cdot L^{-1}$ of fluo-3 pentapotassium salt. The intensity of Fluo-4 or Fluo-3 fluorescence was normalized to the average fluorescence intensity in the images acquired before agonist application and colour coded. The temporal profiles of the agonist-induced $[Ca^{2+}]_i$ transients are illustrated by the plots showing: (i) the time course of the normalized Fluo-4 or Fluo-3 fluorescence intensity (F/F_0) averaged within multiple sub-plasmalemmal regions where F/F_0 changes were initiated and rose above 1.5 or (ii) the time course of F/F_0 averaged within entire confocal optical slice of RVSMC (Gordienko *et al.*, 2008).

Visualization of intracellular calcium stores and the SR

The intracellular calcium stores in RVSMCs were visualized using the low-affinity ($K_{d(Ca)}$ = 42 $\mu mol \cdot L^{-1}$) fluorescent Ca^{2+} indicator fluo-3FF, which was loaded by incubating the myocytes with 5 $\mu mol \cdot L^{-1}$ fluo-3FF AM at room temperature for 90 min followed by a 60 min wash in PSS (Gordienko and Zholos, 2004; Gordienko *et al.*, 2008). The SR was visualized using: (i) ER-Tracker™ Blue-White DPX, which was loaded by incubating the myocytes with 5 $\mu mol \cdot L^{-1}$ of the dye for 40 min; and (ii) Brefeldin A BODIPY 558/568 (Abeele *et al.*, 2006), which was loaded by incubating the myocytes with 2 $\mu mol \cdot L^{-1}$ of the dye for 20 min followed by 1.5 h wash.

Immunostaining of the SR Ca^{2+} release channels

Prior to immunostaining, the SR in RVSMCs was stained with Brefeldin A BODIPY 558/568, as described above. The myocytes were then fixed by incubating them in 4% ($w \cdot v^{-1}$) paraformaldehyde for 15 min. Non-specific binding was blocked by incubating the myocytes with 1% ($w \cdot v^{-1}$) bovine serum albumin (BSA) and 0.3% ($w \cdot v^{-1}$) Triton X-100 (a cell permeabilizing agent) for 1 h at room temperature. Primary and secondary antibodies were diluted in PSS supplemented with 0.3 ($w \cdot v^{-1}$) Triton X-100. To visualize the distribution of IP_3 receptors (IP_3Rs), we used an IP_3R type 1 (IP_3R1)-specific antibody, because IP_3R1 has been shown to be ubiquitous in various tissues (Mackrill *et al.*, 1997; Gordienko and Zholos, 2004; Gordienko *et al.*, 2008) and RT-PCR analysis confirmed expression of gene encoding IP_3R1 in RVSMCs. This antibody was developed (Santa Cruz Biotechnology Inc., Santa Cruz, CA, USA) in goat and has been shown to selectively recognize IP_3R1 in other types of SMCs (Taylor and Traynor, 1995; Gordienko and Zholos, 2004; Gordienko *et al.*, 2008). RyRs were detected with a monoclonal anti-RyR antibody derived (Sigma-Aldrich Co., RBI, Natick, MA, USA) from the 34C hybridoma (produced by the fusion of P3X 63 Ag8.653 myeloma cells and spleen cells from Balb/c mice). This antibody reacts strongly with RyR1, 2 and 3 and was previously used for immunodetection of RyRs in single SMCs (Gordienko and Zholos, 2004; Gordienko *et al.*, 2008). RVSMCs were incubated with primary anti-IP_3R1 or anti-RyR antibodies (both at 1:200 dilution) overnight at 4°C. Following a 10 min rinse (4 times) in PSS, primary antibody-specific binding was detected by incubating the cells for 3 h at room temperature with either donkey anti-goat IgG or goat anti-mouse IgG, both conjugated to MFP 488 (both at 1:400 dilution; MoBiTec, Göttingen, Germany). Prior to confocal imaging the extracellular solution was replaced with Vectashield mounting medium (Vector Laboratories, Inc. Burlingame, CA, USA) containing DAPI for visualization of the cell nucleus. The spatial pattern of the Ca^{2+} release channel distribution was related to the spatial organisation of the SR and nucleus. In controls, incubation with primary antibody was omitted from the experimental protocol.

Confocal microscopy

Experimental chambers with RVSMCs were placed on the stage of either Axiovert 100 M or Axiovert 200 M inverted microscopes attached to a LSM 510 and LSM 510 META laser-scanning units respectively (Zeiss, Oberkochen, Germany). The SCSi interface of the confocal microscopes was hosted by a Pentium PC (32-bit Windows NT 4.0 operating system) running LSM 510 software (Zeiss, Oberkochen, Germany).

During time series protocol, the *x-y* confocal images of Fluo-4 or Fluo-3 fluorescence were acquired at 20–40 Hz using a Zeiss plan-Apochromat 40× 1.3 N.A. oil-immersion objective. Fluo-4 or Fluo-3 fluorescence was excited by the 488 nm line of a 30 mW argon ion laser (Laser-Fertigung, Hamburg, Germany) and was captured at wavelengths above 505 nm. The illumination intensity was attenuated to 0.6–0.7% with an acousto-optical tuneable filter (Zeiss, Oberkochen, Germany). To optimize signal quality, the pinhole was set to provide a confocal optical section below 1.2 µm (measured with 0.2 µm fluorescent beads). The focus was adjusted to acquire the images from the middle of the myocyte depth. In the images acquired in this way, the events initiated within 1 µm of the cell surface (edge) were considered to have sub-plasmalemmal origin and their temporal profiles were analysed (see above).

The imaging of the myocyte structures and spatial distribution of the SR Ca^{2+} release channels was performed using a Zeiss plan-Apochromat 63× 1.4 N.A. oil-immersion objective. The pinhole was set to provide an *x-y* resolution of 0.4 µm

and a confocal optical section (*z* resolution) of 0.8–1 μm (measured with 0.2 μm fluorescent beads). Averaging of four frames was used to reduce a shot noise. To avoid any bleed-through of the fluorescence signal in multistaining experiments, fluorochromes with well-separated excitation and emission spectra were used and imaging was performed using the frame-by-frame multitrack mode of the confocal scanner: sequential acquisition via well-separated optical channels of the *x-y* images produced by fluorescence of different fluorochromes. In these experiments, fluo-4, fluo-3FF and MFP 488 fluorescence were excited by the 488 nm line of a 30 mW argon ion laser and detected at wavelengths of 505–550 nm; ER-Tracker™ Blue-White DPX and DAPI fluorescence were excited by the 405 nm line of a 25 mW laser diode and detected at wavelengths of 420–480 nm; Brefeldin A BODIPY 558/568 was excited by the 543 nm line of a 1 mW helium/neon ion laser and detected at wavelengths above 560 nm. The photomultiplier gain and offset in each optical channel were set individually to achieve similar signal intensity at each channel and remove subsignal noise from the images. The adequacy of the imaging protocol applied to the multi-labelled myocytes was confirmed by control experiments on the monolabelled cells.

Electrophysiological recordings

Electrical recordings from single RVSMCs preloaded with fluo-4 AM (see above) were performed by using perforated-patch (200 μg·mL^{-1} amphotericin B) technique. This allowed low-resistance access to the cell while minimally interfering with $[Ca^{2+}]_i$ (because pores formed by amphotericin B are Ca^{2+}-impermeable). The myocytes were bathed in PSS, dialysed with solution composed of (in mmol·L^{-1}): KCl 115; NaCl 6, HEPES 10 (pH adjusted to 7.4 with KOH), and stimulated with 2 s pulses of 10 μmol·L^{-1} *αβ*-meATP applied at 20 min intervals (see above). Fire-polished borosilicate patch pipettes filled with pipette solution were connected to the head stage of an Axopatch 200A (Molecular Devices Co., Sunnyvale, CA, USA) input amplifier and had a free-tip resistance of 2–5 MΩ. Electrical recordings were synchronized with confocal $[Ca^{2+}]_i$ imaging using a TTL synchronizing pulse generated by the confocal scanner at the beginning of the time series protocol. The electrical signals were filtered at 1 kHz (–3 dB frequency) by four-pole low-pass Bessel filter and digitized at 5 kHz using a DigiData 1200 hosted by a Pentium PC running pCLAMP 6.0 software (Molecular Devices Co., CA, USA).

Flash photolysis

Inositol 1,4,5-trisphosphate was rapidly and uniformly released within RVSMC from D-*myo*-inositol 1,4,5-trisphosphate, $P^{4(5)}$-1-(2-nitrophenyl)ethyl ester trisodium salt ('caged' IP_3) by 1 ms flash of light (300–380 nm) from a xenon arc lamp, as described previously (Gordienko and Zholos, 2004). In these experiments, the myocytes were bathed in PSS and dialysed with solution composed of (in mmol·L^{-1}): KCl 115, NaCl 6, MgATP 5, Li_3GTP 1, HEPES 10 (pH adjusted to 7.4 with KOH) and supplemented with 30 μmol·L^{-1} 'caged' IP_3 and 100 μmol·L^{-1} fluo-3 pentapotassium salt. To ensure equilibration between the pipette solution and cytosol, confocal $[Ca^{2+}]_i$ imaging was commenced at least 5 min after establishment of the whole-cell configuration.

Data analysis and statistical procedures

Image processing was carried out using an Indy workstation (Silicon Graphic, Inc., Mountain View, CA, USA) with custom routines written in IDL (Research Systems, Inc., Boulder, CO, USA). The final figures were produced using MicroCal Origin (MicroCal Software Inc., Northampton, MA, USA) and CorelDraw 7.0 (Corel Corporation, Ottawa, Ontario, Canada). The data are expressed as mean values ± SEM for the number of cells (*n*) analysed. Comparative analysis of the data groups was performed using Student's *t*-test with the threshold for statistical significance set at the 0.05 level.

Drug/molecular target nomenclature

Nomenclature of drugs/molecular targets used in this work conforms to BJP's Guide to Receptors and Channels, 4th edition (Alexander *et al.*, 2009).

Drugs and chemicals

Fluo-4 AM, fluo-3 pentapotassium salt, ER-Tracker™ Blue-White DPX, Brefeldin A BODIPY 558/568 and pluronic F-127 were obtained from Invitrogen Ltd. (Paisley, UK). Fluo-3FF acetoxymethyl ester was from TefLabs (Austin, TA, USA). Donkey anti-goat IgG and goat anti-mouse IgG, both conjugated to MFP 488 were from MoBiTec (Göttingen, Germany). D-*myo*-inositol 1,4,5-trisphosphate, $P^{4(5)}$-1-(2-nitrophenyl)ethyl ester, trisodium salt ('caged' IP_3) was from Calbiochem-Novabiochem (UK) Ltd. (Beeston, Nottingham, UK). *αβ*-meATP trisodium salt, NF279, MRS2578 and (7R)-4-Hydroxy-7-methoxy-N,N,N-trimethyl-3,5,9-trioxa-4-phosphaheptacosan-1-aminium-4-oxide (edelfosine) were from Tocris (Bristol, UK). The RNA extraction kit was purchased from Qiagen (Crawley, UK); the primers and other reagents for RT-PCR experiments were purchased from Invitrogen (Paisley, UK). 1-[6-([(17*β*)-3-methoxyestra-1,3,5(10)-trien-17-yl]amino)hexyl]-1H-pyrrole-2,5-dione (U-73122), 1-[6-([(17*β*)-3-methoxyestra-1,3,5(10)-trien-17-yl]amino)hexyl]-2,5-pyrrolidinedione (U-73343), protease (Type X), collagenase (type 1A), soybean trypsin inhibitor (Type II-S), BSA, ATP (disodium salt), GTP (dilithium salt), creatine, HEPES, 1,3,7-trimethylxanthine (caffeine), dimethyl sulphoxide, paraformaldehyde and Triton X-100 were obtained from Sigma-Aldrich (Poole, UK). All other chemicals were from BDH Laboratory Supplies, AnalaR grade (Pool, UK).

Results

Dependence of $[Ca^{2+}]_i$ transients on P2X receptor agonist concentration

Fluo-4-loaded RVSMCs were stimulated with gradually increasing concentrations of the P2X receptor agonist *αβ*-meATP applied through a glass micropipette as a 2 s pulse (Figure 1A). *αβ*-meATP was applied at 20 min intervals, during which the application pipette was replaced with a new one containing a different concentration of the agonist. The

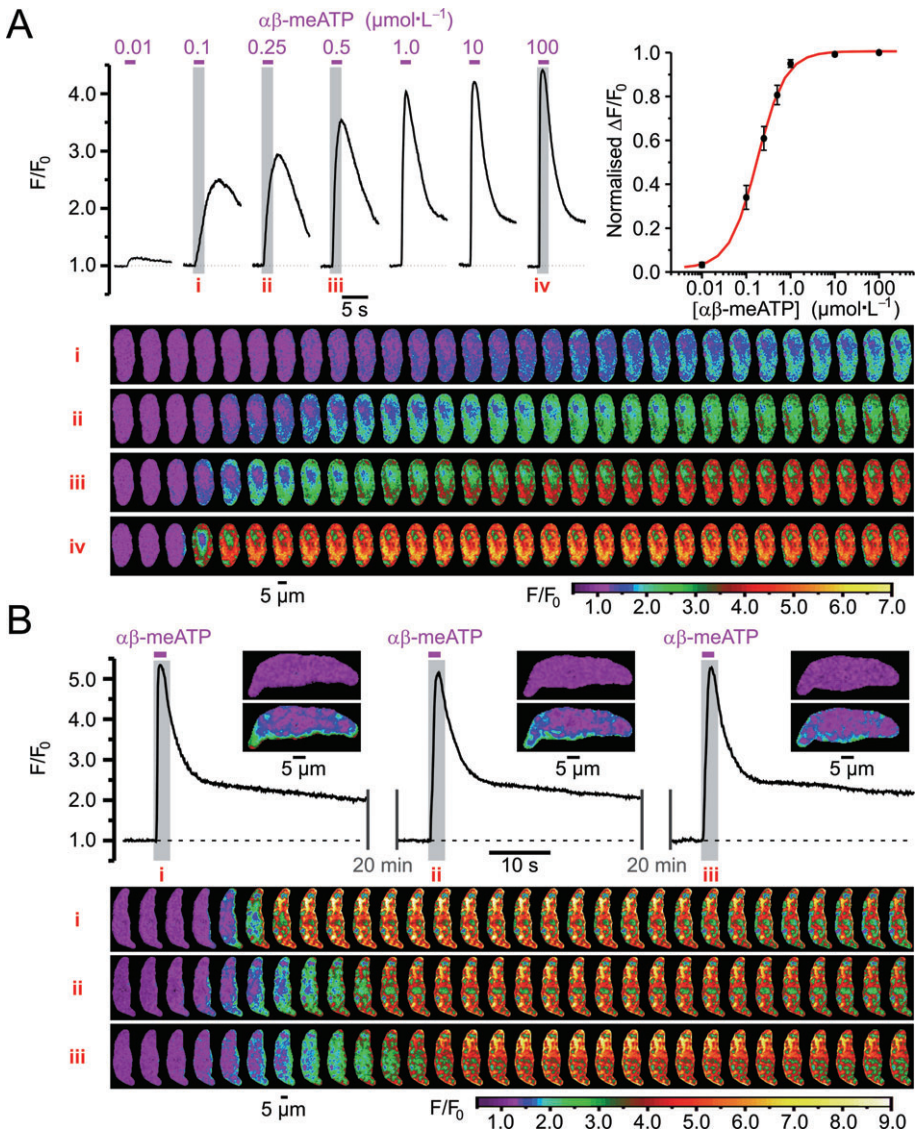

Figure 1

(A) Dependence of $[Ca^{2+}]_i$ transients induced by P2X receptor stimulation in renal vascular smooth muscle cells (RVSMCs) on $\alpha\beta$-methylene ATP ($\alpha\beta$-meATP) concentration. Traces of self-normalized Fluo-4 fluorescence (F/F_0) averaged within confocal (<1.2 μm) slice of the cell reflect $[Ca^{2+}]_i$ transients induced by different $\alpha\beta$-meATP concentrations, as indicated (the drug applications are denoted by magenta bars above the traces, top left). Please note that the traces shown were obtained from two RVSMCs: cell 1 – the responses to 0.1, 0.25, 0.5 and 100 μmol·L^{-1} $\alpha\beta$-meATP and cell 2 – the responses to 0.01, 1.0 and 10 μmol·L^{-1} $\alpha\beta$-meATP. Averaged peaks of $\Delta F/F_0$ transients normalized to that induced by 100 μmol·L^{-1} $\alpha\beta$-meATP in the same cell are plotted versus corresponding $\alpha\beta$-meATP concentrations (top right). Dose–response curve fitted to the data revealed EC_{50} = 0.18 ± 0.01 μmol·L^{-1} (n = 5–10). The four panels (bottom) of 30 colour-coded confocal images were sequentially captured during the periods highlighted in the traces (top left), i–iv respectively. (B) Traces of self-normalized Fluo-4 fluorescence averaged within sub-plasmalemmal regions of initiations (insets) reflect high reproducibility of $[Ca^{2+}]_i$ transients induced by repetitive (with 20 min interval) applications of 10 μmol·L^{-1} $\alpha\beta$-meATP (top). The three panels (bottom) of 30 images were captured during the highlighted periods (top), i–iii respectively.

same RVSMC was stimulated with at least three different agonist concentrations followed by application of 100 μmol·L^{-1} $\alpha\beta$-meATP. The intensity of fluo-4 fluorescence was normalized to that before agonist application and colour-coded. Traces of self-normalized fluo-4 fluorescence (F/F_0) reflect the dynamics of $[Ca^{2+}]_i$ changes induced by different $\alpha\beta$-meATP concentrations (Figure 1A; top left). Each of the four panels in Figure 1 (bottom) show 30 sequential images captured from the same RVSMC following application of 0.1, 0.25, 0.5 and 100 μmol·L^{-1} $\alpha\beta$-meATP (i–iv, respectively) during the periods highlighted in the traces. To quantify the relationship between the response amplitude and $\alpha\beta$-meATP concentration, averaged peaks of $\Delta F/F_0$ transients were normalized to that induced by 100 μmol·L^{-1} $\alpha\beta$-meATP in the same cell and plotted versus $\alpha\beta$-meATP concentrations (Figure 1A; top right). A dose–response curve fitted to the data

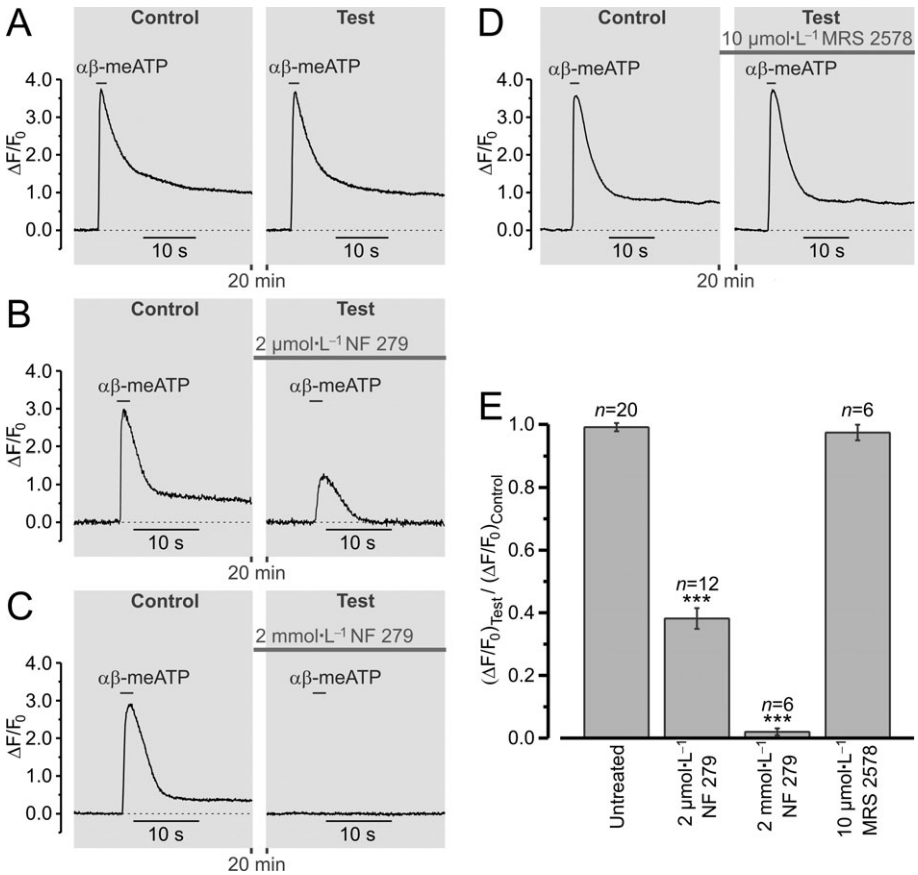

Figure 2

Stimulation of renal vascular smooth muscle cells (RVSMCs) with 10 μmol·L^{-1} $\alpha\beta$-methylene ATP ($\alpha\beta$-meATP) selectively activates P2X receptors. Traces (A–D) of relative changes in Fluo-4 fluorescence ($\Delta F/F_0$) illustrate the experimental protocol. RVSMCs were stimulated with 2 s pulse of $\alpha\beta$-meATP applied twice at a 20 min interval. The peak amplitude of the response ($\Delta F/F_0$) to the second stimulation (Test) was normalized to that of the response to the first stimulation (Control). The Test response was obtained either in the absence an antagonist [A, 'Untreated' in (E)] or following incubation with 2 μmol·L^{-1} (B) or with 2 mmol·L^{-1} (C) of the P2X receptor antagonist NF 279, or with 10 μmol·L^{-1} of the P2Y receptor antagonist MRS 2578 (D). Statistical analysis (E) revealed that the $\alpha\beta$-meATP-induced responses were significantly reduced by NF 279 but were insensitive to MRS 2578. ***$P < 0.001$.

using a non-linear least-squares minimization algorithm revealed EC_{50} = 0.18 ± 0.01 μmol·L^{-1} (n = 5–10). On the one hand, this value is more than six times lower than that which we have recently reported for P2X receptor-mediated current in RVSMCs (Harhun *et al.*, 2010), suggesting that some amplification mechanism contributes to Ca^{2+} mobilization. On the other hand, a gradual increase in the amplitude and rate of rise of the $[Ca^{2+}]_i$ response with increasing $\alpha\beta$-meATP concentration suggests that either no regenerative mechanisms are involved or that these mechanisms are restricted to Ca^{2+} microdomains that function autonomously and are gradually recruited with increasing stimuli (Berridge, 1997). In support of the latter, localized Ca^{2+} events were observed following stimulation with low (≤0.5 μmol·L^{-1}) concentrations of $\alpha\beta$-meATP (Figure 1A; panels i–iii). In response to high (≥1 μmol·L^{-1}) concentrations of $\alpha\beta$-meATP, Ca^{2+} mobilisation was initiated by a sub-plasmalemmal $[Ca^{2+}]_i$ upstroke (SPCU) (Gordienko *et al.*, 2008), an abrupt increase in $[Ca^{2+}]_i$ at multiple sub-plasmalemmal regions, which propagates through the entire cell volume within 300 ms (Figure 1A, panel iv and B, panels i–iii).

To compensate for cell-to-cell variations in Fluo-4 load and/or resting $[Ca^{2+}]_i$ and, thereby, to permit the comparison of findings between different RVSMCs, we evaluated the effect of different drugs on SPCU by relating the fluorescent response ($\Delta F/F_0$) induced by 10 μmol·L^{-1} $\alpha\beta$-meATP in the presence of a drug to that obtained in control in the same myocyte. In these experiments, the same Fluo-4-loaded RVSMCs were stimulated with 2 s pulses of $\alpha\beta$-meATP applied with a 20 min interval. The response to the succeeding stimulation (Test) was related to the response to the first stimulation (Control). The test response was obtained either in control conditions (to evaluate the response reproducibility) or following 20 min incubation with a drug or drug combination. This experimental strategy was validated by high reproducibility of $[Ca^{2+}]_i$ transients induced in control conditions by 10 μmol·L^{-1} $\alpha\beta$-meATP applied at 20 min intervals (Figure 1B, top). On average, the reproducibility of the response amplitude was 99 ± 1% (n = 20) (Figure 2E, 'Untreated' and 7A). Comparing images in the panels also revealed a remarkable constancy of the positions of the sites of initiation of Ca^{2+} mobilization associated with each

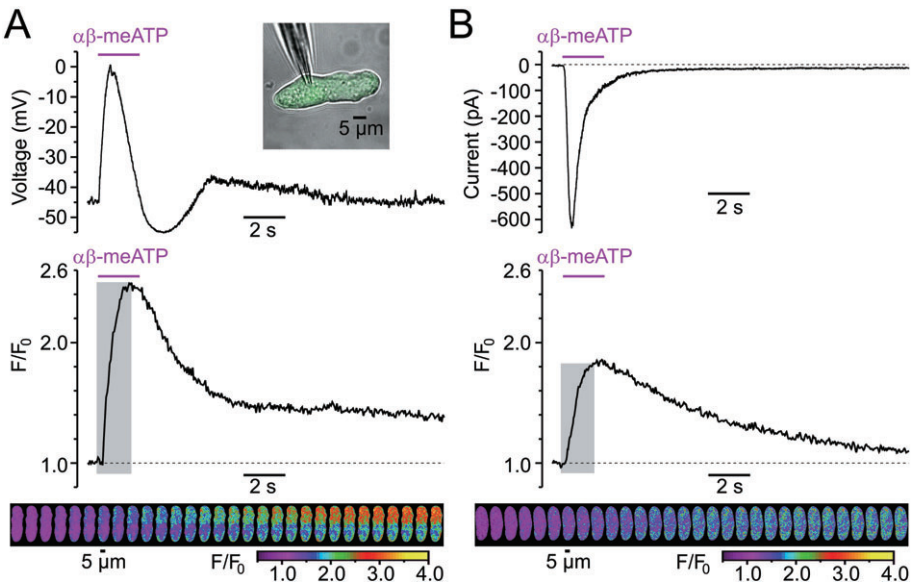

Figure 3

Relationship between the sub-plasmalemmal $[Ca^{2+}]_i$ upstroke (SPCU) induced in renal vascular smooth muscle cells (RVSMCs) by 10 µmol·L^{-1} $\alpha\beta$-methylene ATP ($\alpha\beta$-meATP) and the plasmalemmal electrical events. Changes in the cell membrane potential (A) and transmembrane current at V_h = –60 mV (B) were recorded in Fluo-4-loaded RVSMC using the perforated-patch technique (A, top inset) simultaneously with confocal imaging of $[Ca^{2+}]_i$ changes. In (A) and (B): electrical recordings (top), traces of self-normalized Fluo-4 fluorescence averaged within sub-plasmalemmal regions of initiations (middle), gallery (bottom) of colour-coded (F/F_0) images sequentially captured during the highlighted (middle) periods.

$\alpha\beta$-meATP application (Figure 1B, panels i–iii). This allowed us to analyse SPCU in all subsequent experiments.

The ability of 10 µmol·L^{-1} $\alpha\beta$-meATP to selectively activate P2X receptors was confirmed in separate experiments (Figure 2), where the effects of the P2X receptor antagonist NF 279 and P2Y6 receptor antagonist MRS 2578 on $\alpha\beta$-meATP-induced $[Ca^{2+}]_i$ transients were tested. Of the eight recombinant P2Y receptor subtypes (P2Y1, P2Y2, P2Y4, P2Y6, P2Y11, P2Y12, P2Y13, and P2Y14), only four subtypes were found to be expressed in the kidney: P2Y1, P2Y2, P2Y4 and P2Y6 (reviewed in Guan *et al.*, 2007b). Our RT-PCR analysis of the expression of the genes encoding P2Y receptors performed using single isolated RVSMCs (see *Methods*) revealed the expression of genes encoding only two P2Y receptor subtypes: P2Y2 and P2Y6 (data not shown). Although both of these P2Y receptor subtypes are uridine nucleotide-sensitive rather than adenine nucleotide-sensitive and should not be affected by 10 µmol·L^{-1} $\alpha\beta$-meATP used in this study, we still tested the effect of the P2Y6 receptor antagonist MRS 2578 (as there is no commercially available selective P2Y2 receptor antagonist) on $\alpha\beta$-meATP-induced $[Ca^{2+}]_i$ transients. We found that the peak amplitude of the response ($\Delta F/F_0$) of Fluo-4-loaded RVSMCs to 10 µmol·L^{-1} $\alpha\beta$-meATP was reduced by 61 ± 3% (n = 12) following a 20 min incubation with 2 µmol·L^{-1} NF 279 and by 98 ± 1% (n = 6) following incubation with 2 mmol·L^{-1} NF 279, but was unaffected by 10 µmol·L^{-1} MRS 2578 (n = 6; P = 0.29).

SPCU and plasmalemmal electrical events

Confocal imaging of $[Ca^{2+}]_i$ transients induced in RVSMCs by 10 µmol·L^{-1} $\alpha\beta$-meATP was combined with electrical recordings performed using the perforated patch technique (Gordienko *et al.*, 2008). Under current clamp (Figure 3A), SPCU was associated with a spike-like depolarization, which reached a peak of –2.8 ± 1.0 mV within 90 ± 15 ms (n = 14). Only three out of 14 RVSMCs revealed an overshoot (3.2 ± 1.1 mV). This suggests that the $\alpha\beta$-meATP-induced depolarization is mainly caused by the P2X receptor-mediated rather than VGCC-mediated current. Concurrent elevation of $[Ca^{2+}]_i$ peaked within 792 ± 35 ms (n = 14) and persisted after recovery of the membrane potential to the resting level, thus, implying that mechanisms other than P2X-mediated Ca^{2+} entry contribute to the intracellular Ca^{2+} mobilization.

When the same RVSMC was voltage-clamped (at –60 mV), P2X receptor activation did not induce depolarization of the cell membrane, thus preventing a contribution of VGCCs to the $\alpha\beta$-meATP-induced response. Under these conditions, the peak of the Fluo-4 response ($\Delta F/F_0$) was reduced by 43% (Figure 3B). On average, the peak of the $\alpha\beta$-meATP-induced response ($\Delta F/F_0$) detected under voltage-clamp conditions was reduced by 37 ± 4% (n = 14) relative to that detected under current-clamp conditions. This statistically significant reduction (P < 0.00008; paired t-test) suggests that Ca^{2+} entry through VGCCs contributes to the $\alpha\beta$-meATP-induced SPCU. Under voltage-clamp conditions P2X-mediated inward current reached a peak within 106 ± 18 ms, while concurrent SPCU peaked within 1508 ± 40 ms (n = 14). This discrepancy suggests that Ca^{2+} release from the SR is recruited following P2X receptor activation. Indeed, even though VGCCs were not activated under these conditions, the elevation of $[Ca^{2+}]_i$ continued to advance when the P2X-mediated current started to decline. Deceleration of the

SPCU resulting from VGCC deactivation implies that the SR Ca^{2+} release can be speeded up by Ca^{2+} entry through VGCCs. Thus, under voltage-clamp conditions, when depolarization of the cell membrane by P2X receptor-mediated current does not occur, the link between P2X receptor activation and Ca^{2+} entry via VGCCs is lost and $[Ca^{2+}]_i$ mobilization evoked by P2X receptor activation is substantially distorted. Therefore, all subsequent experiments were conducted on non-clamped myocytes.

Contribution of voltage-gated Ca^{2+} entry and the SR Ca^{2+} release to SPCU

In these experiments, nicardipine was applied 30 s before $\alpha\beta$-meATP to minimize the possible effect of VGCC block on the SR calcium load. The ability of the external application of 5 $\mu mol \cdot L^{-1}$ nicardipine to completely block VGCCs within 16 s was confirmed in separate voltage-clamp experiments (n = 5; data not shown). The effects of blocking VGCCs following calcium store depletion (Figure 4A) and calcium store depletion following block of VGCCs (Figure 4B) on SPCU induced by 10 $\mu mol \cdot L^{-1}$ $\alpha\beta$-meATP were tested. Incubation of RVSMCs for 20 min with 50 $\mu mol \cdot L^{-1}$ cyclopiazonic acid (CPA), an inhibitor of the sarco-/endoplasmic reticulum Ca^{2+}-ATPase (SERCA), which has no direct effect on VGCCs, Ca^{2+}-dependent K^+ channels or voltage-dependent K^+ channels (Suzuki *et al.*, 1992), completely depleted intracellular calcium stores in RVSMCs, as assessed with 5 $mmol \cdot L^{-1}$ caffeine (n = 9; data not shown). The fraction of the calcium store depletion induced by a single application of 5 $mmol \cdot L^{-1}$ caffeine was estimated in RVSMCs pre-incubated for 5 min with 10 $\mu mol \cdot L^{-1}$ CPA (to inhibit SERCA without the calcium store depletion) and was found to be 94 ± 2% (n = 12; data not shown), thus confirming that 5 $mmol \cdot L^{-1}$ is a sufficient concentration of caffeine to test the SR Ca^{2+} content in these cells. Depletion of calcium stores by a 20 min incubation with 50 $\mu mol \cdot L^{-1}$ CPA reduced the peak of the $\alpha\beta$-meATP-induced response ($\Delta F/F_0$) by 53%. Subsequent block of VGCCs with 5 $\mu mol \cdot L^{-1}$ nicardipine (while keeping calcium stores depleted) resulted in an additional reduction of the peak response by 20% (Figure 4A). The peak response was attenuated by 44% following block of VGCCs alone, and was reduced further by 10% following subsequent calcium store depletion (Figure 4B). These observations suggest that both Ca^{2+} entry through VGCCs and the SR Ca^{2+} release contribute to the SPCU. The response persisting in the presence of both nicardipine and CPA arose from Ca^{2+} entry though P2X receptors and had a peak amplitude 29 ± 3% of that in control (n = 20).

To assess the role of Ca^{2+} entry through VGCCs in the activation of the SR Ca^{2+} release, we compared the effect of calcium store depletion following block of VGCCs with that observed in the absence of nicardipine (Figure 4C). This experimental strategy (illustrated by traces obtained from two other RVSMCs) revealed that in control conditions calcium store depletion reduced the response ($\Delta F/F_0$) to $\alpha\beta$-meATP by 53 ± 3% (n = 22), while when VGCCs were blocked, the calcium store depletion decreased the response by only 23 ± 5% (n = 8). Significant attenuation of the effect of the calcium store depletion on the SPCU following block of VGCCs implies that Ca^{2+} release from the SR following P2X receptor activation is induced mainly by Ca^{2+} entry through VGCCs.

Contribution of RyRs and IP_3Rs to the SR Ca^{2+} release following P2X receptor activation

Ryanodine receptors activity was assessed with 100 $\mu mol \cdot L^{-1}$ ryanodine, a highly selective agent, which at micromolar concentrations blocks RyR-mediated Ca^{2+} release without calcium store depletion (Sutko *et al.*, 1997; Janiak *et al.*, 2001; Gordienko and Bolton, 2002) and does not affect IP_3Rs (Janiak *et al.*, 2001) or VGCCs (Balke and Wier, 1991). IP_3R activity was assessed with 30 $\mu mol \cdot L^{-1}$ 2-aminoethoxydiphenyl borate (2-APB). Because it was previously suggested that 2-APB may affect mechanisms of intracellular Ca^{2+} homeostasis other than those mediated by IP_3R, including inhibition of store-operated Ca^{2+} entry and SERCA (reviewed by Bootman *et al.*, 2002), we tested the effect of 30 $\mu mol \cdot L^{-1}$ 2-APB on the SR calcium load and Ca^{2+} entry mechanisms evoked by P2X receptor activation in RVSMCs (Figure 5).

P2X receptor-mediated current (Figure 5A) was unaffected by a 10 min incubation with 30 $\mu mol \cdot L^{-1}$ 2-APB (n = 5). To unmask Ca^{2+} entry induced by P2X receptor stimulation in RVSMCs, the intracellular calcium stores were depleted by at least 20 min incubation with 50 $\mu mol \cdot L^{-1}$ CPA prior to stimulation with 10 $\mu mol \cdot L^{-1}$ $\alpha\beta$-meATP (Figure 5B). Under these experimental conditions, $\alpha\beta$-meATP-induced $[Ca^{2+}]_i$ transients were insensitive to 30 $\mu mol \cdot L^{-1}$ 2-APB (n = 9). The SR calcium load, assessed with 5 $mmol \cdot L^{-1}$ caffeine (Figure 5C), was also unaffected by the 20 min incubation with 30 $\mu mol \cdot L^{-1}$ 2-APB (n = 8). These observations validate 30 $\mu mol \cdot L^{-1}$ 2-APB as a selective probe for IP_3R-mediated Ca^{2+} release in RVSMCs.

To analyse the contribution of RyRs and IP_3Rs to the SR Ca^{2+} release evoked by P2X receptor activation, the effects of successive cumulative inhibition of IP_3Rs after RyRs (Figure 6A) and RyRs after IP_3Rs (Figure 6B) on SPCU induced by 10 $\mu mol \cdot L^{-1}$ $\alpha\beta$-meATP were tested. Block of RyRs reduced the peak of the response ($\Delta F/F_0$) to $\alpha\beta$-meATP by only 18%. Subsequent inhibition of IP_3Rs resulted in an additional reduction of the response by 57% (Figure 6A). The response was attenuated by 60% following inhibition of IP_3Rs alone, and reduced further by 8% following subsequent block of RyRs (Figure 6B).

An important condition of the above strategy is the ability of 100 $\mu mol \cdot L^{-1}$ ryanodine to block RyRs without calcium store depletion. This was tested in separate experiments. In these experiments (Figure 6C, left: top panel), after 20 min incubation with 100 $\mu mol \cdot L^{-1}$ ryanodine the RVSMCs were stimulated with 10 $\mu mol \cdot L^{-1}$ $\alpha\beta$-meATP twice. The $\alpha\beta$-meATP pulses were applied at 20 min intervals. The amplitude of the $[Ca^{2+}]_i$ transient induced by the second $\alpha\beta$-meATP application (Test) was related to that induced by the first one (Control). On average, the reproducibility of the amplitude of the response to 10 $\mu mol \cdot L^{-1}$ $\alpha\beta$-meATP in the presence of 100 $\mu mol \cdot L^{-1}$ ryanodine was found to be 98 ± 5% (n = 6) (Figure 6, right); this was not statistically different (P = 0.778) from that observed in RVSMCs not treated with ryanodine, 99 ± 1% (n = 20) (Figure 2E). This observation indicates that, with the experimental protocol used in this study,

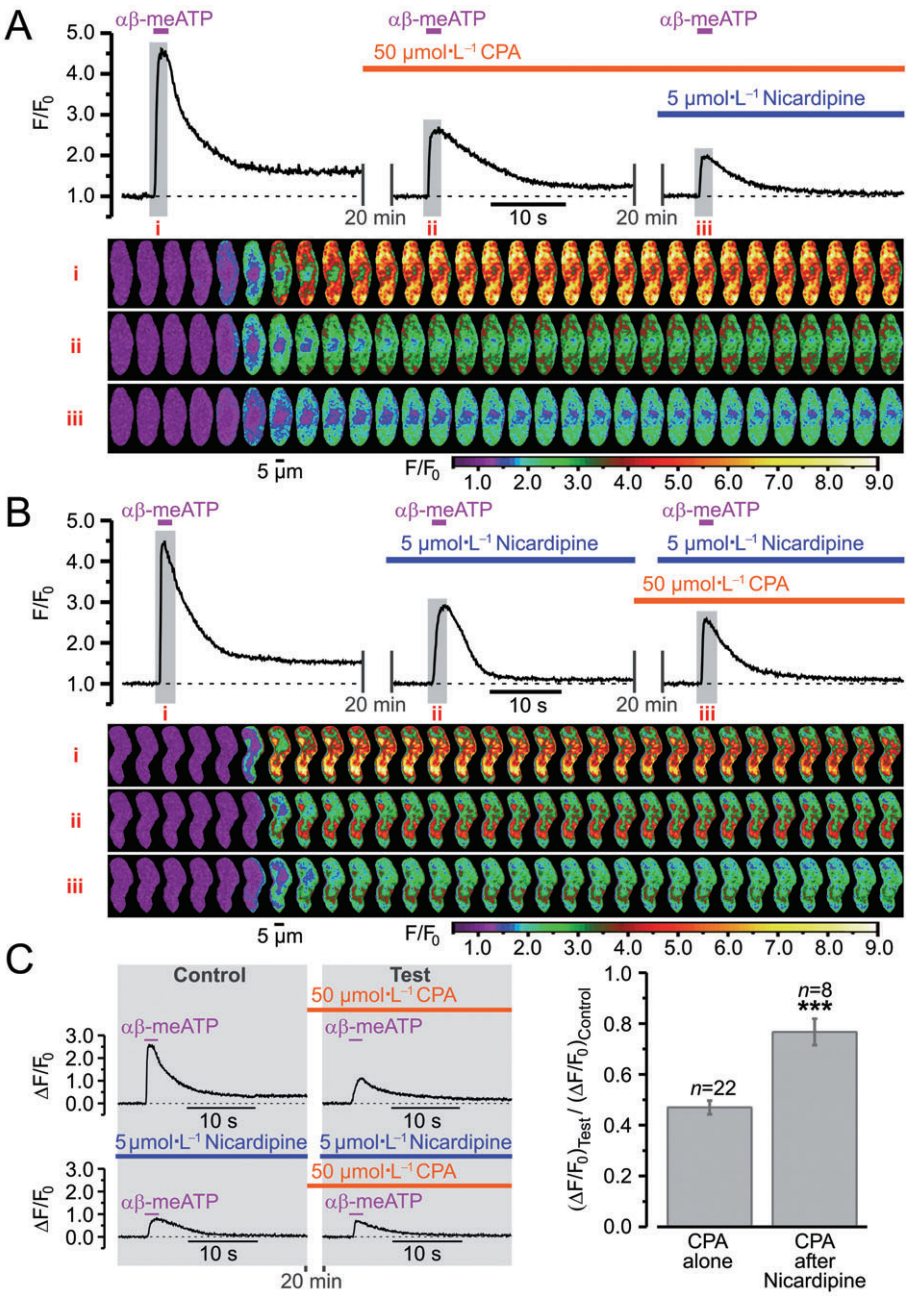

Figure 4

Ca^{2+} entry via voltage-gated Ca^{2+} channels (VGCCs) following P2X receptor activation in renal vascular smooth muscle cells (RVSMCs) induces Ca^{2+} release from intracellular calcium stores. Effect of (A) block of VGCCs (with 5 µmol·L^{-1} nicardipine) following calcium store depletion (by 20 min incubation with 50 µmol·L^{-1} cyclopiazonic acid, CPA) and (B) calcium store depletion following block of VGCCs on SPCU triggered by repetitive (with 20-min interval) applications of 10 µmol·L^{-1} $\alpha\beta$-methylene ATP ($\alpha\beta$-meATP). The panels below the traces of self-normalized Fluo-4 fluorescence show colour-coded (F/F_0) confocal images sequentially captured during the periods highlighted in the traces, i–iii respectively. (C) The amplitude of $\Delta F/F_0$ transients detected following calcium store depletion (Test) was normalized to that detected before incubation with CPA (Control) before and following block of VGCCs (left) and compared (right). ***$P < 0.001$.

100 µmol·L^{-1} ryanodine blocks RyR-mediated Ca^{2+} release without depleting the calcium store.

Ryanodine receptors and IP$_3$Rs are both Ca^{2+}-sensitive and may activate each other via CICR mechanism (Fill and Copello, 2002; Foskett *et al.*, 2007). Thus, by blocking one receptor type the effect of CICR on the other receptor type will also be lost. To eliminate the effect of possible cross-activation of these receptors from the analysis, the responses ($\Delta F/F_0$) to $\alpha\beta$-meATP in the presence of both blockers were normalized to the responses in the presence of each blocker alone and compared (Figure 6C). This revealed that when RyRs were initially blocked, inhibition of IP$_3$Rs reduced the

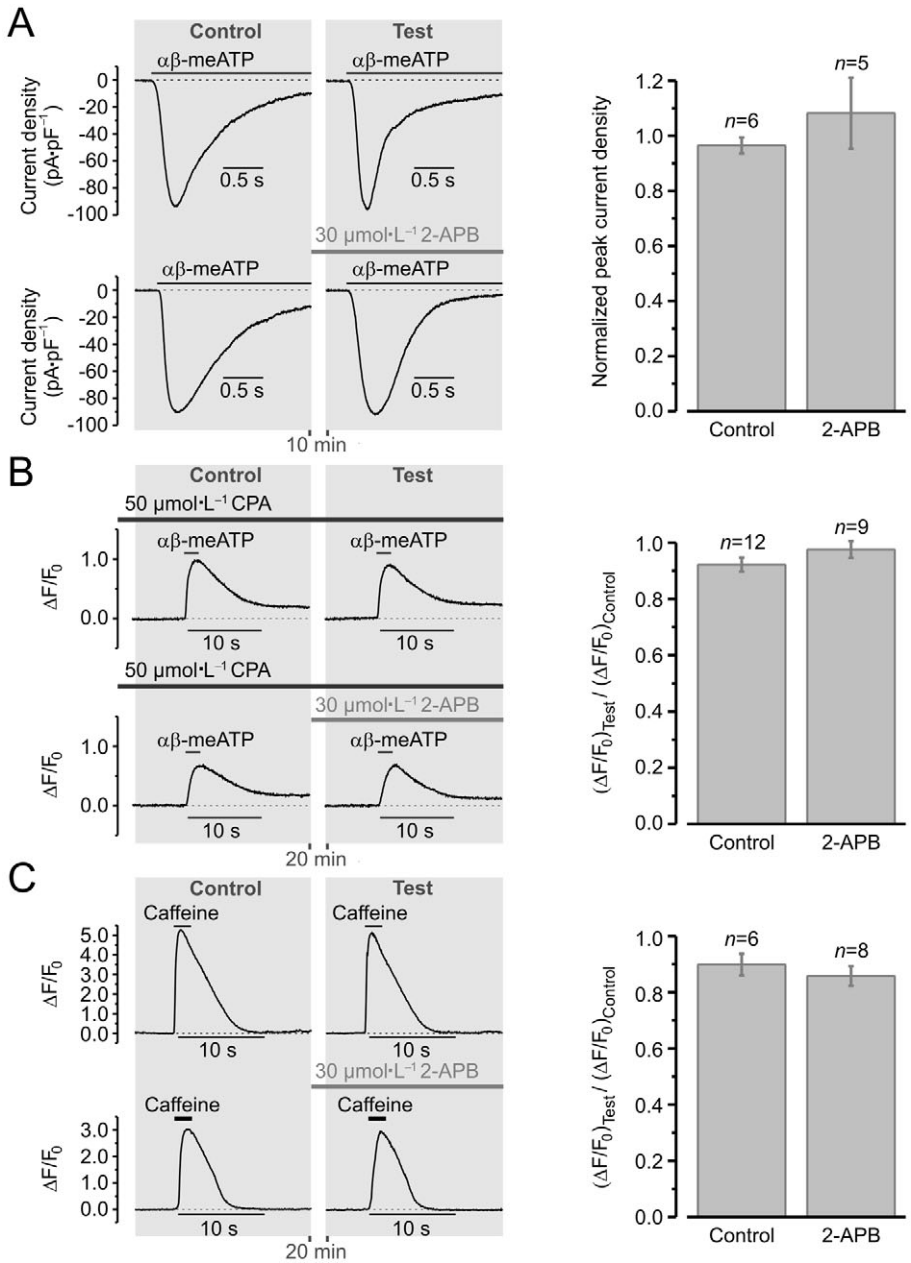

Figure 5

2-aminoethoxydiphenyl borate (2-APB) (30 μmol·L^{-1}) exerts no effect on (A) the P2X receptor-mediated cationic current (B) the Ca^{2+} entry mechanisms induced by P2X receptor activation and (C) the sarcoplasmic reticulum (SR) calcium load. Left panels (in A–C) illustrate experimental protocols. Renal vascular smooth muscle cells were stimulated with 2 s pulses of 10 μmol·L^{-1} $\alpha\beta$-methylene ATP ($\alpha\beta$-meATP) (A, B) or 5 mmol·L^{-1} caffeine (C) applied twice from a glass micropipette at 10-min (A) or 20-min (B, C) intervals and the peak amplitude of the responses was measured: (A) current density and (B, C) relative changes in Fluo-4 fluorescence ($\Delta F/F_0$). Depleting the calcium store by at least 20 min incubation with 50 μmol·L^{-1} CPA unmasked Ca^{2+} entry induced by P2X receptor stimulation (B). The peak amplitude of the response ($\Delta F/F_0$) to caffeine reflects the SR calcium load (C). The peak amplitude of the response to the second application of the agonist (Test) was normalized to that of the response to the first application of the agonist (Control) in each case (A–C). The Test response was obtained either in the absence of 2-APB (to asses reproducibility of the response to the agonist) or following incubation with 30 μmol·L^{-1} 2-APB (to assess the effect of the drug). Statistical analysis (right panels in A–C), revealed no significant effect of 30 μmol·L^{-1} 2-APB: $P = 0.36$ (A), $P = 0.28$ (B) and $P = 0.45$ (C).

response by 61 ± 4% ($n = 7$). In contrast, when IP_3Rs were initially blocked, inhibition of RyRs reduced the response by only 20 ± 3% ($n = 5$). This suggests that Ca^{2+} release from the SR following P2X receptor activation is mediated mainly by IP_3Rs.

Figure 7 summarizes the effects of VGCC/SERCA/RyR/IP_3R/PLC inhibitors on the SPCU induced in RVSMCs by 10 μmol·L^{-1} $\alpha\beta$-meATP. The analysis strategy was the same as described above. The response to the succeeding stimulation (Test) was related to the response to the first stimulation

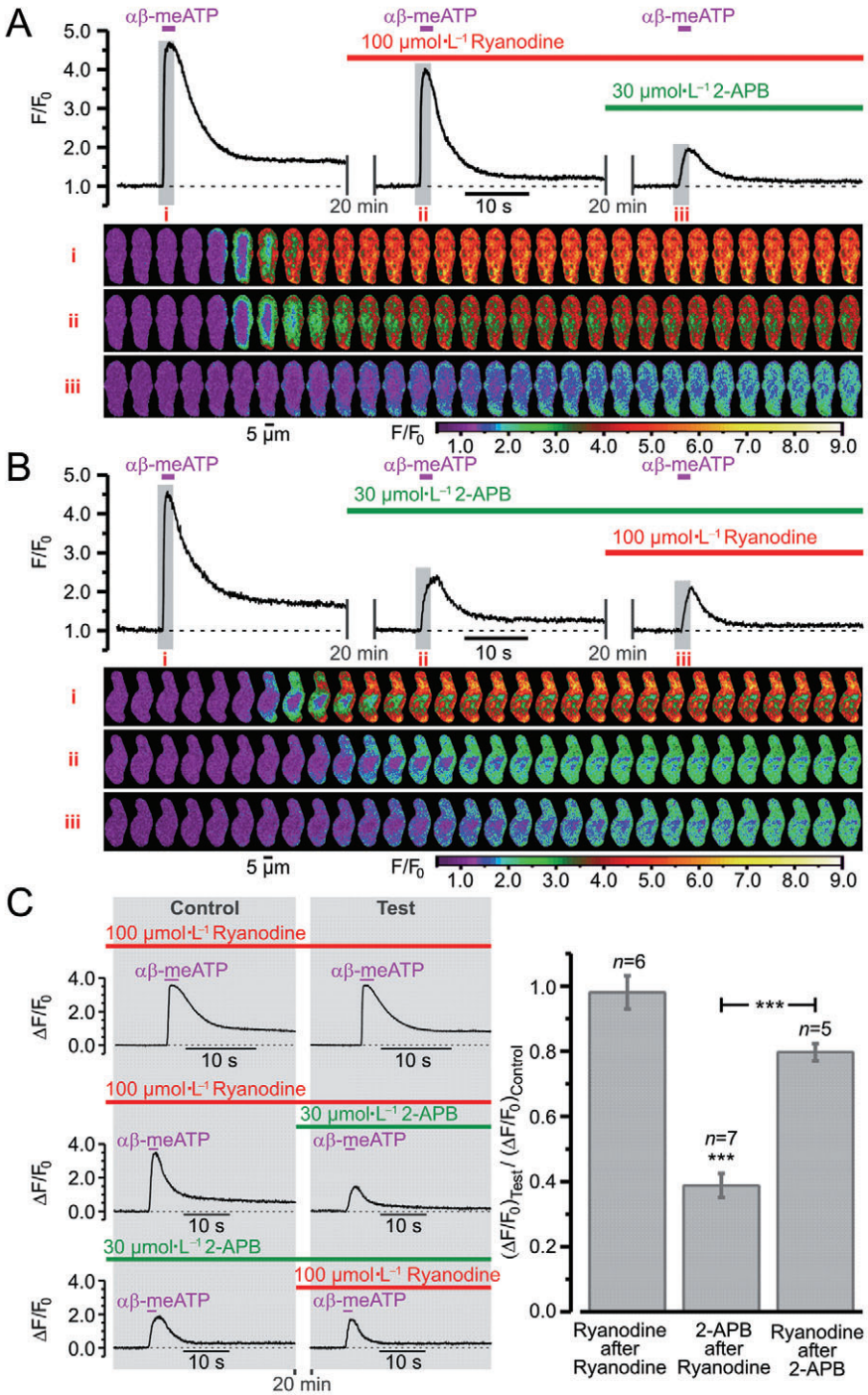

Figure 6

Relative contribution of ryanodine receptor (RyR)- and inositol 1,4,5-trisphosphate receptor (IP$_3$R)-mediated Ca^{2+} release to sub-plasmalemmal $[Ca^{2+}]_i$ upstroke (SPCU) induced by P2X receptor activation in renal vascular smooth muscle cells. Effect of successive cumulative inhibition of (A) IP$_3$Rs [with 30 µmol·L^{-1} 2-aminoethoxydiphenyl borate (2-APB)] after RyRs (with 100 µmol·L^{-1} ryanodine) and (B) RyRs after IP$_3$Rs on SPCU triggered by repetitive applications of 10 µmol·L^{-1} $\alpha\beta$-methylene ATP ($\alpha\beta$-meATP). The cells were incubated with the Ca^{2+} release channel inhibitors for 20 min before the application of $\alpha\beta$-meATP. The panels below the traces of self-normalized Fluo-4 fluorescence show colour-coded confocal images sequentially captured during the periods highlighted in the traces, i–iii respectively. (C) The peak amplitude of the response to the second application of the agonist (Test) was normalized to that of the response to the first application of the agonist (Control). The Test response was obtained either in the presence of ryanodine alone (to assess possible effect of ryanodine on the calcium store load; left: top panel) or in the presence of both 2-APB and ryanodine (to asses the cumulative effect of the drugs; left: middle and bottom panels). The amplitudes of $\Delta F/F_0$ transients detected in the presence of the two inhibitors were normalized to that detected in the presence of one of them and in both cases were compared (right). ***$P < 0.001$.

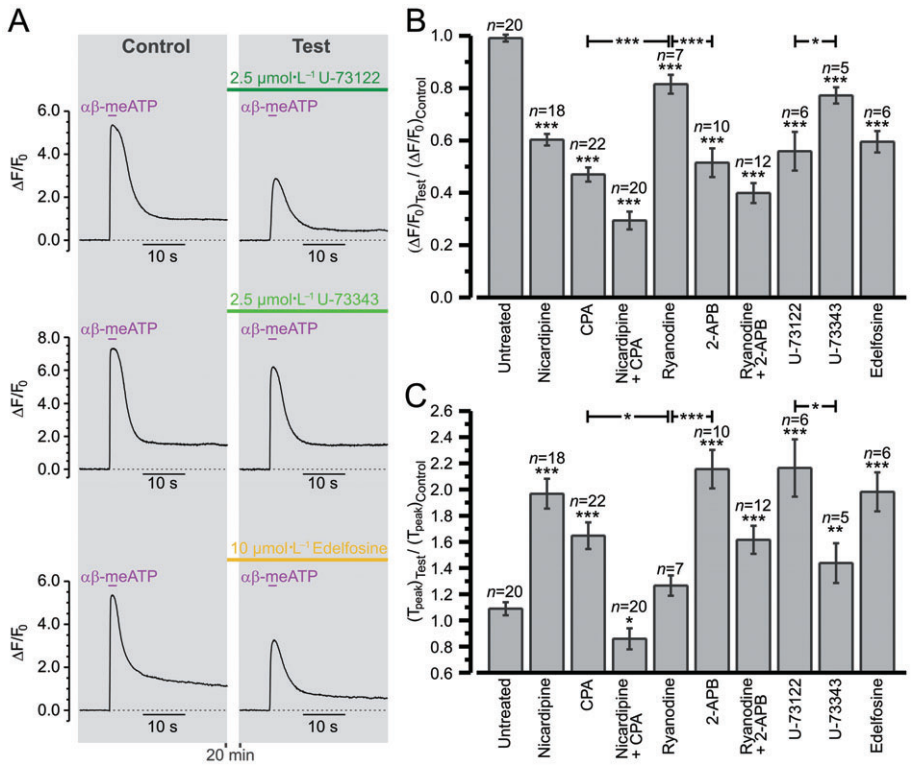

Figure 7

Summary of the effects of voltage-gated Ca^{2+} channel/sarco-/endoplasmic reticulum Ca^{2+}-ATPase/ryanodine receptor/inositol 1,4,5-trisphosphate receptor/phospholipase C inhibitors on sub-plasmalemmal $[Ca^{2+}]_i$ upstroke in renal vascular smooth muscle cells (RVSMCs). Experimental protocol is illustrated in (A). Fluo-4 loaded RVSMCs were stimulated with 2 s pulses of 10 μmol·L^{-1} $\alpha\beta$-methylene ATP ($\alpha\beta$-meATP) applied with a 20 min interval. The response ($\Delta F/F_0$ averaged at sub-plasmalemmal regions of initiation) to the second stimulation (Test) was related to the response to the first stimulation (Control). The Test response was obtained either in control conditions ('Untreated') or following incubation with a drug or drug combination. Two parameters were examined and summarized: (B) relative change in peak amplitude and (C) relative change in time-to-peak. *P < 0.05, **P < 0.01 and ***P < 0.001 versus control, unless denoted otherwise. 2-APB, 2-aminoethoxydiphenyl borate; CPA, cyclopiazonic acid.

(Control). The test response was obtained either in control conditions (to evaluate the response reproducibility) or following 20 min incubation with a drug or drug combination. Figure 7A shows sample traces illustrating this experimental protocol. Relative changes in the response peak amplitude (Figure 7B) and time-to-peak (Figure 7C) were analysed. In control conditions ('Untreated'), the amplitude and time-to-peak of the test response constituted 99 ± 1% and 109 ± 5% of the control response respectively (n = 20). Block of RyRs (100 μmol·L^{-1} ryanodine) reduced the amplitude by only 18 ± 4% (n = 7) and had no significant effect on time-to-peak (P = 0.08). The effect of IP_3R inhibition (30 μmol·L^{-1} 2-APB) was significantly stronger: reduction of the amplitude by 48 ± 6% and increase of the time-to-peak by 98 ± 15% (n = 10). The effect of calcium store depletion (20 min incubation with 50 μmol·L^{-1} CPA) was also significantly stronger than that of RyR inhibition: reduction of the amplitude by 53 ± 3% and increase of the time-to-peak by 51 ± 10% (n = 22). The effect of simultaneous block of RyRs and IP_3Rs was similar to the effect of calcium store depletion: reduction of the amplitude by 60 ± 4% and increase of the time-to-peak by 48 ± 11% (n = 12). Block of VGCCs (5 μmol·L^{-1} nicardipne) reduced the amplitude by 39 ± 2% and increased time-to-peak by 81 ± 11% (n = 18). Block of VGCCs following calcium store depletion reduced the amplitude by 70 ± 3% and decreased time-to-peak by 21 ± 8% (n = 20). It should be noted that calcium store depletion (with CPA) reduced the $\alpha\beta$-meATP-induced response significantly (P < 0.0006) more than block of VGCCs, suggesting that Ca^{2+} release from the SR is partially induced by Ca^{2+} entering the cell via P2X receptors. Calcium store depletion with simultaneous block of VGCCs reduced the response significantly (P < 0.0002) more than calcium store depletion alone, suggesting that Ca^{2+} entry via VGCCs makes a significant contribution to the $\alpha\beta$-meATP-induced Ca^{2+} mobilization. Comparison of mean amplitudes of the responses ($\Delta F/F_0$) to $\alpha\beta$-meATP in RVSMCS with depleted calcium stores obtained in the absence and in the presence of nicardipine suggests that the Ca^{2+} influx via P2X receptors is ~1.8 times larger than that via VGCCs. Thus, Ca^{2+} influx following P2X receptor activation induces Ca^{2+} release from the SR, which is mediated mainly (but not solely) via IP_3Rs and accelerates intracellular Ca^{2+} mobilization.

While P2X receptors do not signal via phospholipase C-β (PLC-β), basal levels of $[IP_3]_i$ produced by spontaneous activity of PLC (Prestwich and Bolton, 1991; Gordienko and Bolton, 2002; Horowitz *et al.*, 2005; Peng *et al.*, 2007) may

play a permissive role in activation of IP_3R-mediated Ca^{2+} release by voltage-gated Ca^{2+} entry. Although the rates of hydrolysis by G_q-activated PLC-β are accelerated by elevation of $[Ca^{2+}]_i$, the results of experiments on permeabilized cells have suggested that $[Ca^{2+}]_i$ levels achieved during cell signalling do not activate PLC-β by themselves but are required for PLC-β activation by G_q (Fisher *et al.*, 1989; Horowitz *et al.*, 2005). Thus, it is unlikely that $\alpha\beta$-meATP-induced $[Ca^{2+}]_i$ mobilization could *per se* activate PLC-β. Activation of any $G_{q/11}$-coupled receptors in RVSMCs by 10 $\mu mol \cdot L^{-1}$ $\alpha\beta$-meATP is also unlikely, because the $\alpha\beta$-meATP-induced $[Ca^{2+}]_i$ transients were completely abolished by selective P2X antagonist NF 279, but were unaffected by P2Y antagonist MRS 2578 (see Figure 2). Nevertheless, we tested the effect of commercially available PLC inhibitors on the $\alpha\beta$-meATP-induced $[Ca^{2+}]_i$ transients. The aminosteroid compound U-73122 and its relatively inactive analogue U-73343 (Smith *et al.*, 1990) both significantly reduced the amplitude and increased the time-to-peak of the response (Figure 7B and C). However, the effect of 2.5 $\mu mol \cdot L^{-1}$ U-73122 (the reduction of the amplitude by 44 ± 7% and increase of the time-to-peak by 99 ± 22%; n = 6) was significantly stronger than that of 2.5 $\mu mol \cdot L^{-1}$ U-73343 (the reduction of the amplitude by 22 ± 3% and increase of the time-to-peak by 32 ± 15%; n = 5). Although these compounds are known to have many side effects attributable to alkylation of various proteins (Horowitz *et al.*, 2005), the difference between the effect of U-73122 and that of U-73343 suggests a permissive role of IP_3 in activation of IP_3Rs by Ca^{2+} in RVSMCs. To test this further, we examined the effect of another PLC inhibitor, the ether lipid analogue edelfosine (Powis *et al.*, 1992; Horowitz *et al.*, 2005). Preincubation with 10 $\mu mol \cdot L^{-1}$ edelfosine (Figure 7) reduced the amplitude of the $\alpha\beta$-meATP-induced $[Ca^{2+}]_i$ transients by 40 ± 4% and increased time-to-peak by 82 ± 11% (n = 6). We therefore concluded that the ability of Ca^{2+} entering the RVSMCs following P2X receptor stimulation to induce IP_3R-ediated Ca^{2+} release depends on $[IP_3]_i$ which is determined by spontaneous basal activity of PLC.

To assess the role of Ca^{2+} entry through VGCCs in IP_3R activation, we compared the effect of IP_3R inhibition following block of VGCCs with that observed in the absence of nicardipine (Figure 8). This experimental strategy was validated by high reproducibility of the responses to 10 $\mu mol \cdot L^{-1}$ $\alpha\beta$-meATP in the presence of 30 $\mu mol \cdot L^{-1}$ 2-APB (Figure 8A). The effect of IP_3R inhibition on the SPCU was attenuated by block of VGCCs (Figure 8B). To quantify this, the responses ($\Delta F/F_0$) in the presence of 2-APB were normalized to the responses before IP_3R inhibition, both in control and in the presence of nicardipine, and compared (Figure 8C). This revealed that, when VGCCs were initially blocked, IP_3R inhibition decreases the response by only 16 ± 4% (n = 12), while in control conditions (without pretreatment with nicardipine) IP_3R inhibition reduced the response ($\Delta F/F_0$) to $\alpha\beta$-meATP by 48 ± 6% (n = 10). Significant attenuation of the effect of IP_3R inhibition on SPCU by block of VGCCs implies that IP_3R-mediated Ca^{2+} release is induced mainly (but not solely; see above) by Ca^{2+} influx via VGCCs.

Sub-plasmalemmal SR is enriched with IP_3Rs

Tight functional coupling between VGCCs and IP_3Rs suggests the expression of IP_3Rs in jSR. Intracellular calcium stores, visualized in RVSMCs with the low-affinity Ca^{2+} indicator Fluo-3FF, coincided with SR elements, visualized with ER-Tracker Blue-White or Brefeldin A BODIPY (n = 27), and consisted of some central elements and a sub-plasmalemmal SR network (Figure 9A). Similar organization of the SR has been reported in other SMC types (Gordienko *et al.*, 2001; 2008; Gordienko and Zholos, 2004). RT-PCR analysis of single RVSMCs revealed the expression of genes encoding IP_3R type 1 and RyR type 2 (Figure 9B). Immunodetection of IP_3Rs and RyRs in RVSMCs stained with Brefeldin A BODIPY and DAPI (Figure 9C) revealed that type 1 IP_3Rs are primarily expressed in sub-plasmalemmal SR elements (n = 21), while RyRs predominate in deeper SR, particularly in the perinuclear region of the myocyte (n = 16). Based on this distribution of IP_3Rs and RyRs, Ca^{2+} responses to stimuli selectively targeting IP_3Rs and RyRs are expected to initiate from different positions within the cell. In the same RVSMC loaded with Fluo-4 and stained with ER-Tracker (Figure 9D), the sites of initiation of $\alpha\beta$-meATP-induced response coincide with positions of subplasmalemmal SR elements, while the site of initiation of the response to caffeine (which selectively activates RyR-mediated Ca^{2+} release) coincides with the position of deeper central SR elements (n = 8), as evident from a comparison of the images number 2 in the panels (Figure 9D, bottom) showing sequential images captured during the initial phase of the response to $\alpha\beta$-meATP (left) and caffeine (middle). Furthermore, flash release of IP_3 (which selectively activates IP_3Rs) within the entire cell volume (Figure 9D) initiated Ca^{2+} release at the cell periphery (n = 5), similar to P2X receptor stimulation.

Discussion

The nature of mechanisms coupling excitation to $[Ca^{2+}]_i$ elevation, as well as the spatial organization and molecular composition of intracellular Ca^{2+} release units are important determinants of the contractile response in all types of muscles (Berridge, 1997; Wier and Balke, 1999; Lamb, 2002; Blatter *et al.*, 2003; Wang *et al.*, 2004; McCarron *et al.*, 2006). In skeletal muscles, excitation triggers Ca^{2+} release from the SR via protein–protein interactions between VGCCs and RyRs (Lamb, 2002). In cardiac muscles, Ca^{2+} entry through VGCCs triggers RyR-mediated Ca^{2+} release via CICR mechanism (Wier and Balke, 1999; Blatter *et al.*, 2003; Wang *et al.*, 2004). In both cases, the structural basis for E–C coupling is close juxtaposition of the SR RyRs and VGCCs. In smooth muscles, elevation of $[Ca^{2+}]_i$ is caused either by cell membrane depolarization (electromechanical coupling; Somlyo and Somlyo, 1968) leading to opening of VGCCs, which are manifested by the generation of action potentials or allow Ca^{2+} to 'leak' into the cell giving rise to 'sparklets' (Amberg *et al.*, 2007), or by activation of metabotropic receptors (pharmacomechanical coupling; Somlyo and Somlyo, 1968) usually linked to $G_{q/11}$-GTP/PLC/IP_3/IP_3R-mediated Ca^{2+} release, or by a combination of these mechanisms (Bolton *et al.*, 1999; Davis and Hill, 1999). The initial Ca^{2+} mobilization may be augmented by RyR-mediated Ca^{2+} release recruited via a CICR mechanism (Bolton and Gordienko, 1998; Bayguinov *et al.*, 2000; White and McGeown, 2002; Kotlikoff, 2003; Zhang *et al.*, 2003; Hotta *et al.*, 2007; Gordienko *et al.*, 2008). The contribution of

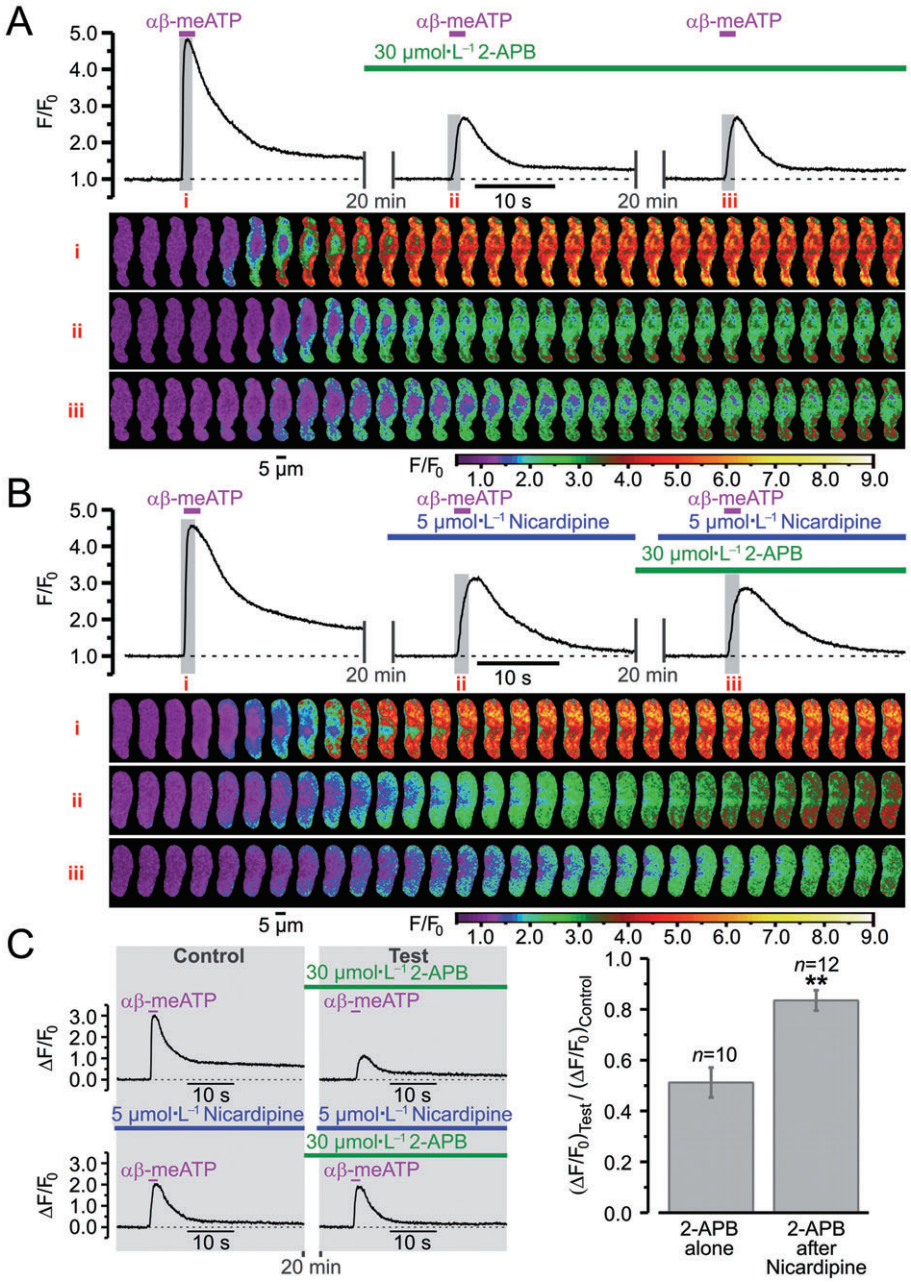

Figure 8

Relative contribution of P2X receptor- and voltage-gated Ca^{2+} channel (VGCC)-mediated Ca^{2+} entry to activation of inositol 1,4,5-trisphosphate receptor (IP_3R)-mediated Ca^{2+} release in renal vascular smooth muscle cells. Effect of IP_3R inhibition (A) and IP_3R inhibition after block of VGCCs (B) on sub-plasmalemmal $[Ca^{2+}]_i$ upstroke triggered by repeated applications of 10 μmol·L^{-1} $\alpha\beta$-methylene ATP ($\alpha\beta$-meATP). The panels below the traces of self-normalized Fluo-4 fluorescence show colour-coded (F/F_0) confocal images sequentially captured during the periods highlighted in the traces, i–iii respectively. (C) The amplitude of $\Delta F/F_0$ transients detected following IP_3R inhibition (Test) was normalized to that detected before incubation with 2-aminoethoxydiphenyl borate (2-APB) (Control), both without (left, top panel) and in the presence of nicardipine (left, bottom panel), and compared (right). $^{**}P < 0.01$.

these mechanisms to intracellular Ca^{2+} mobilization may vary in different SMC types, depending on the type and strength of stimuli, SMC excitability and spatial organisation of intracellular Ca^{2+} release units (Walsh, 1994; Bolton and Gordienko, 1998; Bolton *et al.*, 1999; Davis and Hill, 1999; Bayguinov *et al.*, 2000; Gordienko *et al.*, 2001, 2008; Janiak *et al.*, 2001; Gordienko and Bolton, 2002; White and McGeown, 2002; Kotlikoff, 2003; Wier and Morgan, 2003; Zhang *et al.*, 2003; Lamont and Wier, 2004; McCarron *et al.*, 2006; Amberg *et al.*, 2007; Hotta *et al.*, 2007; Wier *et al.*, 2009).

We hypothesized that in vascular myocytes Ca^{2+} entry following activation of ionotropic P2X receptors may

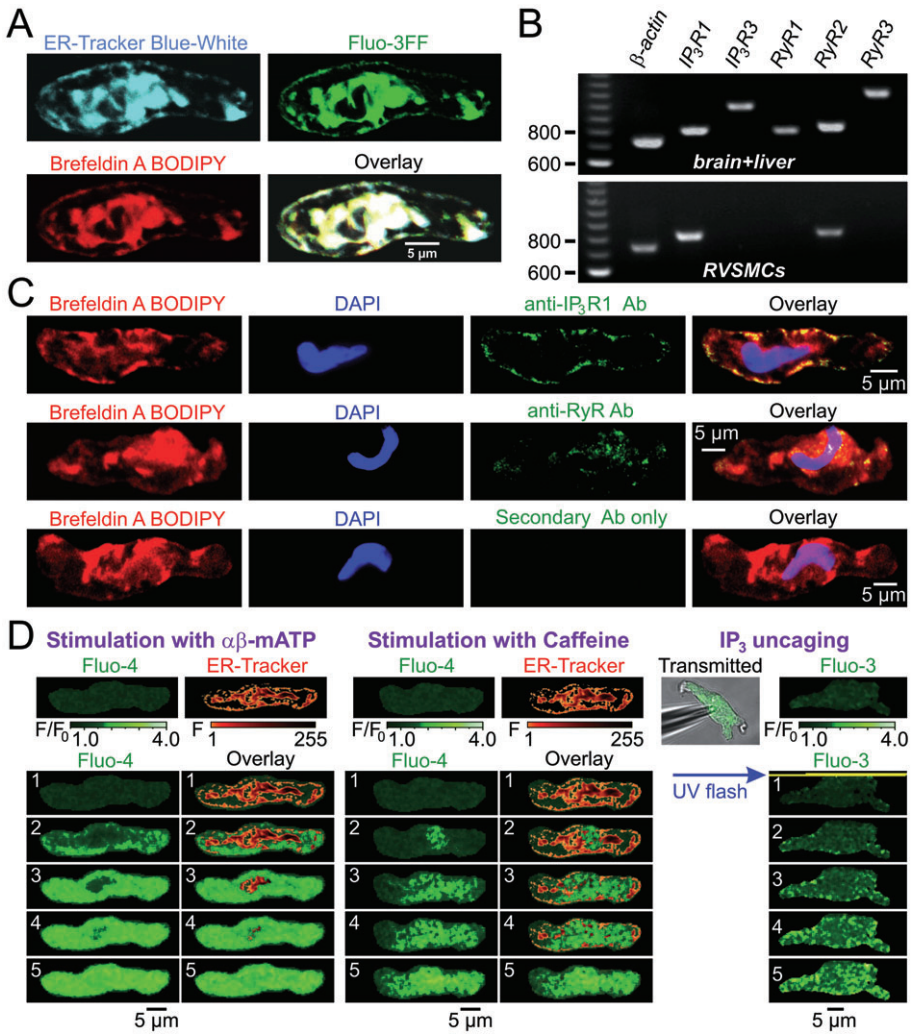

Figure 9

Spatial distribution of the sarcoplasmic reticulum (SR) Ca^{2+} release channels in renal vascular smooth muscle cells (RVSMCs). (A) Confocal images of the ER-tracker Blue-White, Fluo-3FF and Brefeldin A BODIPY fluorescence, and their overlay illustrate spatial organization of the SR in RVSMC. (B) RT-PCR analysis of inositol 1,4,5-trisphosphate receptor (IP_3R) and ryanodine receptor (RyR) expression in RVSMCs. Primers designed to amplify genes encoding IP_3R and RyR subtypes: IP_3R1 (806 bp), IP_3R3 (966 bp), RyR1 (793 bp), RyR2 (824 bp), RyR3 (1086 bp) were tested for their specificity using cDNA preparations of rat brain and liver tissue (top) before using them on RVSMC preparations (bottom). RVSMCs were found to express genes encoding IP_3R1 and RyR2. (C) Immunodetection of IP_3R1 (top) and RyR (middle) in RVSMC stained with Brefeldin A BODIPY and DAPI. Primary antibody binding was detected with MFP488-conjugated secondary antibody, which shows no non-specific binding in the absence of primary antibody (bottom). Confocal images highlight localization of IP_3R1 in sub-plasmalemmal SR and RyR in deeper SR. (D) RVSMCs were either pre-incubated with Fluo-4AM and ER-tracker Blue-White (pseudocolour confocal images) and stimulated sequentially with 10 $\mu mol \cdot L^{-1}$ $\alpha\beta$-methylene ATP ($\alpha\beta$-meATP) (left) or 5 $mmol \cdot L^{-1}$ caffeine (middle), or loaded with Fluo-3 and 'caged' IP_3 via patch pipette (transmitted light and confocal images) and stimulated by whole-cell UV flash (right). Galleries of five sequential images (labelled 1–5, bottom) highlight spatial patterns of the initial phase of the responses.

induce IP_3R-mediated Ca^{2+} release. Our hypothesis was based on the following findings reported in visceral and vascular myocytes: (i) a localized increase in $[Ca^{2+}]_i$ induced by local flash release of Ca^{2+} from a 'caged' precursor may trigger IP_3R-mediated Ca^{2+} release (Ji *et al.*, 2006); (ii) Ca^{2+} entry via VGCCs facilitates IP_3R-mediated Ca^{2+} release following stimulation of metabotropic receptors (Gordienko *et al.*, 2008); (iii) the stoichiometric ratio of RyRs to IP_3Rs in SMCs is 1:9–10, suggesting the existence of a Ca^{2+}-storage compartment devoid of RyRs but equipped with IP_3Rs (Wibo and Godfraind, 1994); (iv) caffeine/ryanodine-releasable and IP_3-releasable calcium stores in the SR of vascular myocytes are at least partially distinct with about 56% of the SR being solely IP_3-sensitive (Blaustein *et al.*, 2002); and (v) visualization of Ca^{2+} release sites recruited by selective IP_3R stimulation and IP_3R immunodetection in single SMCs suggests that they are predominantly expressed in sub-plasmalemmal SR (Bayguinov *et al.*, 2000; Zhang *et al.*, 2003; Gordienko and Zholos, 2004; Gordienko *et al.*, 2008).

It should be noted, however, that there is no general agreement about the calcium store arrangement in SMCs. Indeed, the results of early experiments conducted on permeabilized strips of portal vein, pulmonary artery and taenia caeci suggested the existence of two separate calcium stores: S_α expressing both RyRs and IP_3Rs and S_β expressing only IP_3Rs. The contribution of the S_β store to IP_3-induced Ca^{2+} release was estimated to be 60% in taenia caecum, 40% in pulmonary artery and only 6% in portal vein (reviewed in Wray and Burdyga, 2010). In contrast, the results of more recent experiments conducted on isolated pulmonary artery myocytes suggested that IP_3-releasable and caffeine-releasable calcium stores are virtually completely separate (Janiak *et al.*, 2001). A similar conclusion was made from the experiments performed on in intact precapillary vessels, where agonist-induced $[Ca^{2+}]_i$ oscillations were insensitive to the combined action of caffeine and ryanodine (Borisova *et al.*, 2009). An elegant study recently conducted by Rainbow *et al.* (2009) on guinea-pig hepatic portal vein myocytes provided strong evidence for the existence of a single luminally continuous SR where the opening of IP_3Rs and RyRs is regulated by luminal $[Ca^{2+}]$, so that when the luminal $[Ca^{2+}]$ declines, the receptor opening also declines and stops. This model therefore suggests that the appearance of multiple stores in some functional studies may arise from the regulation of luminal $[Ca^{2+}]$ by RyRs and IP_3Rs expressed in a single luminally continuous SR.

We tested our hypothesis that Ca^{2+} entry following P2X activation may induce IP_3R-mediated Ca^{2+} release on RVSMCs, because: (i) P2X receptors mediate sympathetic control and autoregulation of the renal circulation (Malpas and Leonard, 2000; Nishiyama *et al.*, 2000; Bell *et al.*, 2003; Inscho *et al.*, 2003; Cupples and Braam, 2007; Guan *et al.*, 2007a; Surprenant and North, 2009); and (ii) RVSMCs express functional monomeric P2X1 and heteromeric P2X1/4 receptors (Harhun *et al.*, 2010).

We found that depolarization of RVSMC induced by selective stimulation of P2X receptors with $\alpha\beta$-meATP triggers Ca^{2+} release from sub-plasmalemmal SR enriched with IP_3Rs but poor in RyRs, similar to direct stimulation of IP_3Rs by uniform cell-wide release of IP_3 from its 'caged' precursor. The $\alpha\beta$-meATP-induced SPCU was significantly reduced by block of VGCCs or depletion of the intracellular calcium stores, indicating that activation of P2X receptors in RVSMCs recruits both voltage-gated Ca^{2+} entry and the SR Ca^{2+} release to intracellular Ca^{2+} mobilization. Activation of voltage-gated Ca^{2+} influx through L-type Ca^{2+} channels following P2X receptor stimulation was previously demonstrated in preglomerular microvascular SMCs of rat kidney (White *et al.*, 2001). However, the involvement of the SR Ca^{2+} release mechanisms was not addressed in that study. Also, $[Ca^{2+}]_i$ transients induced by 10 μmol·L^{-1} $\alpha\beta$-meATP in preglomerular microvascular SMCs were completely abolished by 20 μmol·L^{-1} NF 279, while in RVSMCs from interlobar and arcuate arteries 2 mmol·L^{-1} NF 279 reduced the $[Ca^{2+}]_i$ transients by 98%. This discrepancy may arise from variations in the distribution of P2X receptor subtypes in SMCs from different regions of renal vascular bed and may reflect the contribution of heteromeric P2X1/4 and monomeric P2X4 receptors to intracellular Ca^{2+} mobilization in RVSMCs from interlobar and arcuate arteries (Harhun *et al.*, 2010). Here we not only demonstrated that the SR Ca^{2+} release is recruited following P2X receptor activation, but also provided strong evidence suggesting that this release is mediated mainly by IP_3Rs. Indeed, depletion of calcium stores, block of VGCCs or IP_3Rs reduced the amplitude and rate of rise of $\alpha\beta$-meATP-induced SPCU significantly more than block of RyRs. This implies that Ca^{2+} entry following P2X receptor activation induces IP_3R-mediated Ca^{2+} release which serves to accelerate $[Ca^{2+}]_i$ elevation and is initiated at sub-plasmalemmal SR enriched with IP_3Rs but poor in RyRs.

It is unlikely that stimulation of RVSMCs with 10 μmol·L^{-1} $\alpha\beta$-meATP recruited any metabotropic receptors coupled to a $G_{q/11}$/PLC/IP_3 signalling pathway, because the $\alpha\beta$-meATP-induced $[Ca^{2+}]_i$ transients were completely abolished by the selective P2X antagonist NF 279, but were unaffected by the P2Y antagonist MRS 2578. Even though activation of PLC-β by G_q is accelerated at $[Ca^{2+}]_i$ levels achieved during cell signalling, direct activation of PLC-β by Ca^{2+} is also unlikely (Fisher *et al.*, 1989; Horowitz *et al.*, 2005). Nevertheless, the effect of PLC-β inhibition with either U-73122 or edelfosine on $\alpha\beta$-meATP-induced $[Ca^{2+}]_i$ transients in RVSMCs was not statistically different from that of IP_3R inhibition with 2-APB. This suggests that basal levels of $[IP_3]_i$ produced by spontaneous activity of PLC (Prestwich and Bolton, 1991; Gordienko and Bolton, 2002; Horowitz *et al.*, 2005; Peng *et al.*, 2007) may play a permissive role in the activation of IP_3R-mediated Ca^{2+} release by elevated $[Ca^{2+}]_i$ achieved following P2X receptor activation. It should be noted, however, that U-73122 is known for its side effects attributable to alkylation of various proteins (Horowitz *et al.*, 2005), while edelfosine appears to be cytotoxic causing cell swelling and eventual lysis, and therefore may well have its own side effects (Horowitz *et al.*, 2005). Indeed, out of the16 RVSMCs tested, edelfosine caused lysis of four myocytes and induced substantial elevation of $[Ca^{2+}]_i$ in five cells.

A comparison of the effect of the calcium store depletion with the cumulative effect of the calcium store depletion and block of VGCCs revealed that, following stimulation of RVSMCs with 10 μmol·L^{-1} $\alpha\beta$-meATP, P2X receptors contributed more than VGCCs to Ca^{2+} entry. This is consistent with the high density of P2X receptor-mediated currents in RVSMCs (Harhun *et al.*, 2010) and high Ca^{2+} permeability of P2X1 and P2X4 receptors: a relative Ca^{2+} over Na^+ permeability (P_{Ca}/P_{Na}) of 4.8 and 4.2 was reported for P2X1 and P2X4 receptors respectively (North, 2002; Egan *et al.*, 2006). Nevertheless, IP_3R-mediated Ca^{2+} release was activated mainly by Ca^{2+} entering the cell via VGCCs. Indeed, the effect of IP_3R inhibition on the SPCU was reduced by threefold following block of VGCCs. This suggests the co-localization of plasmalemmal VGCCs and the jSR IP_3Rs, and 'local control' (Berridge, 1997; McCarron *et al.*, 2006) of Ca^{2+} release mechanisms in RVSMCs. The latter is also supported by the gradual dependence of $[Ca^{2+}]_i$ transients on $\alpha\beta$-meATP concentration, despite the fact that a regenerative CICR mechanism was recruited (Arendshorst and Thai, 2009). The validation of this hypothesis, however, requires a separate electron microscopy study of 'Ca^{2+} release units' (Moore *et al.*, 2004) in RVSMCs.

It is now generally accepted that jSR (which lies within 12–15 nm of plasmalemma), the overlying plasmalemma microdomains and the intervening, tiny volume of cytosol form junctional complexes that serve as the Ca^{2+} 'buffer

barrier', through which Ca^{2+} can move directly between the extracellular fluid and jSR (Blaustein *et al.*, 2002; Poburko *et al.*, 2008). This may facilitate (i) local elevation of luminal $[Ca^{2+}]$ in jSR; and (ii) accumulation of molecules, including Ca^{2+}, Na^+ (Blaustein *et al.*, 2002; Poburko *et al.*, 2008), and IP_3, in the cytosolic microvolume from which the diffusion into the bulk cytoplasm is markedly restricted (Poburko *et al.*, 2008). Taking this into account, the following factors may favour activation of IP_3Rs by Ca^{2+} influx: (i) a robust increase in $[Ca^{2+}]_i$ in the junctional cytosolic microvolume (Blaustein *et al.*, 2002; Poburko *et al.*, 2008); (ii) spontaneous basal activity of PLC (Prestwich and Bolton, 1991; Gordienko and Bolton, 2002; Horowitz *et al.*, 2005; Peng *et al.*, 2007); (iii) Ca^{2+} activation of type 1 IP_3Rs with positive co-operativity (Foskett *et al.*, 2007); (iv) regulation of IP_3Rs by the SR luminal $[Ca^{2+}]$ (Rainbow *et al.*, 2009); and (v) IP_3R clustering (Rahman and Taylor, 2009).

It should be noted, however, that the precise evaluation of the relative contribution of Ca^{2+} entry (P2X receptors and VGCCs) and Ca^{2+} release (IP_3Rs and RyRs) mechanisms to $\alpha\beta$-meATP-induced $[Ca^{2+}]_i$ transients is limited by: (i) a non-linear relationship between the intensity of the indicator fluorescence and $[Ca^{2+}]_i$; and (ii) the possible effects of pharmacological agents targeting the SR Ca^{2+} release mechanisms (either via the SR calcium load or via inhibition of IP_3Rs/RyRs) on the cell membrane potential and, hence, the population of VGCCs available for activation by P2X receptor-mediated depolarization and/or the initial driving force for Ca^{2+} entry. The ability of calcium store modulators (CPA, ryanodine and 2-APB) to alter the cell membrane potential is usually attributed to their effect on spontaneous RyR- and/or IP_3R-mediated Ca^{2+} release events, which modulate the cell membrane potential via activation of Ca^{2+}-dependent K^+ channels and/or Ca^{2+}-dependent Cl^- channels (Burdyga and Wray, 1999; Gordienko *et al.*, 1999; Bayguinov *et al.*, 2000; Hashitani and Brading, 2003; Hashitani *et al.*, 2006; Zizzo *et al.*, 2006; von der Weid *et al.*, 2008; ZhuGe *et al.*, 1998; 2010). Since spontaneous Ca^{2+} release events were observed in less than 5% of RVSMCs used in this study, it is rather unlikely that inhibition of the SR Ca^{2+} release by ryanodine, 2-APB or CPA had any significant effect on resting membrane potential in these myocytes. Also, there is no evidence in the literature for a direct effect (which can be evaluated only from the single channel activity in isolated patches) of the calcium store modulators on potassium and/or chloride channels. On the contrary, it was demonstrated that neither ryanodine (Sakai *et al.*, 1988) nor CPA (Suzuki *et al.*, 1992) had any direct effect on Ca^{2+}-dependent K^+ channels in SMCs. In this study we have demonstrated that in RVSMCs 2-APB exerts no effect on the Ca^{2+} entry mechanisms induced by P2X receptor activation and the SR calcium load (Figure 5). Because the effect of 2-APB on $\alpha\beta$-meATP-induced $[Ca^{2+}]_i$ transient was significantly attenuated in the presence of nicardipine, we concluded that in RVSMCs IP_3R-mediated Ca^{2+} release following P2X receptor stimulation is activated mainly by Ca^{2+} entering the cell via VGCCs.

Although activation of the SR Ca^{2+} release by Ca^{2+} entering the cell via VGCCs has been demonstrated in voltage-clamp experiments performed on different types of visceral and vascular SMCs (Kamishima and McCarron, 1997; Kohda *et al.*, 1997; Bolton and Gordienko, 1998; Shmigol *et al.*, 1998; Coussin *et al.*, 2000), there is a number of studies (e.g. Bradley *et al.*, 2002; 2004) demonstrating that complete depletion of the SR of Ca^{2+} (including IP_3-sensitive store) does not reduce $[Ca^{2+}]_i$ transients induced by step-like depolarization of the cell membrane. The latter results suggest that CICR is not recruited. An alternative explanation given by Bradley *et al.* (2004) suggests that the SR and sarcolemma may form a passive physical barrier to Ca^{2+} influx ('a Ca^{2+} trap'), which normally limits the $[Ca^{2+}]_i$ rise occurring during depolarization. The drugs, which open the SR Ca^{2+} release channels and facilitate the SR Ca^{2+} leak, diminish the influence of 'the Ca^{2+} trap' and may, thereby, increase the amplitude of $[Ca^{2+}]_i$ transients resulting from Ca^{2+} entry via VGCCs even when the SR contains little or no Ca^{2+} (Bradley *et al.*, 2004).

In cardiac myocytes, abnormal intracellular Ca^{2+} handling arising from altered expression/function of RyRs and/or IP_3Rs promotes arrhythmias, atrial fibrillation and heart failure (George and Lai, 2007; Kockskämper *et al.*, 2008). In vascular myocytes, mechanisms coupling P2X receptor activation to IP_3R-mediated Ca^{2+} release may be altered in hypertension. Indeed, it was demonstrated that impaired Ca^{2+} signalling attenuates P2X receptor-mediated vasoconstriction of afferent arterioles in angiotensin II hypertension (Zhao *et al.*, 2005). On the other hand, elevated PLC-β levels and activity were reported in renal arterioles of young spontaneously hypertensive rats (Peng *et al.*, 2007) and were suggested to account for previously demonstrated exaggerated renal vasoconstriction and Ca^{2+} signalling in preglomerular arterioles induced by angiotensin II, thromboxane A_2 and vasopressin in spontaneously hypertensive versus normotensive rats (Feng and Arendshorst, 1997; Iversen and Arendshorst, 1999; Vagnes *et al.*, 2005).

To conclude, we demonstrated that P2X receptor activation evokes IP_3R-mediated Ca^{2+} release in RVSMCs, which is induced mainly by voltage-gated Ca^{2+} entry. This mechanism provides convergence of signalling pathways engaged in electromechanical and pharmacomechanical coupling in smooth muscles of renal vasculature and should be taken into consideration when developing new therapeutic strategies. Further work, however, is needed to examine whether and how this mechanism is altered in hypertension.

Acknowledgements

Supported by British Heart Foundation grants (PG/08/062/25382 and FS/06/077).

Conflicts of interest

None.

References

Abeele FV, Bidaux G, Gordienko D, Beck B, Panchin YV, Baranova AV *et al.* (2006). Functional implications of calcium permeability of the channel formed by Pannexin 1. J Cell Biol 174: 535–546.

Alexander SP, Mathie A, Peters JA (2009). Guide to Receptors and Channels (GRAC), 4th Edition. Br J Pharmacol 158 (Suppl. 1): S1–S254.

Amberg GC, Navedo MF, Nieves-Cintron M, Molkentin JD, Santana LF (2007). Calcium sparklets regulate local and global calcium in murine arterial smooth muscle. J Physiol 579: 187–201.

Arendshorst WJ, Thai TL (2009). Regulation of the renal microcirculation by ryanodine receptors and calcium-induced calcium release. Curr Opin Nephrol Hypertens 18: 40–49.

Balke CW, Wier WG (1991). Ryanodine does not affect calcium current in guinea pig ventricular myocytes in which Ca^{2+} is buffered. Circ Res 68: 897–902.

Bayguinov O, Hagen B, Bonev AD, Nelson NT, Sanders KM (2000). Intracellular calcium events activated by ATP in murine colonic myocytes. Am J Physiol 279: C126–C135.

Bell PD, Lapointe JY, Sabirov R, Hayashi S, Peti-Peterdi J, Manabe K *et al.* (2003). Macula densa cell signaling involves ATP release through a maxi anion channel. Proc Natl Acad Sci USA 100: 4322–4327.

Berridge MJ (1997). Elementary and global aspects of calcium signalling. J Physiol 499: 291–306.

Blatter LA, Kockskämper J, Sheehan KA, Zima AV, Hüser J, Lipsius SL (2003). Local calcium gradients during excitation-contraction coupling and alternans in atrial myocytes. J Physiol 546: 19–31.

Blaustein MP, Golovina VA, Song H, Choate J, Lencesova L, Robinson SW *et al.* (2002). Organization of Ca^{2+} stores in vascular smooth muscle: functional implications. In: Chadwick DJ, Goode JA (eds). Role of the Sarcoplasmic Reticulum in Smooth Muscle. John Wiley & Sons Ltd.: Sussex, pp. 125–137.

Boittin FX, Coussin F, Macrez N, Mironneau G, Mironneau J (1998). Inositol 1,4,5-trisphosphate and ryanodine-sensitive Ca^{2+} release channel-dependent Ca^{2+} signalling in rat portal vein. Cell Calcium 23: 303–311.

Boittin FX, Macrez N, Halet G, Mironneau J (1999). Norepinephrine-induced Ca^{2+} waves depend on $InsP_3$ and ryanodine receptor activation in vascular myocytes. Am J Physiol 277: C139–C151.

Bolton TB, Gordienko DV (1998). Confocal imaging of calcium release events in single smooth muscle cells. Acta Physiol Scand 164: 567–575.

Bolton TB, Prestwich SA, Zholos AV, Gordienko DV (1999). Excitation-contraction coupling in gastrointestinal and other smooth muscles. Annu Rev Physiol 61: 85–115.

Bootman MD, Cheek TR, Moreton RB, Bennett DL, Berridge MJ (1994). Smoothly graded Ca^{2+} release from inositol 1,4,5-trisphosphate-sensitive Ca^{2+} stores. J Biol Chem 269: 24783–24791.

Bootman MD, Collins TJ, Mackenzie L, Roderick HL, Berridge MJ, Peppiatt CM (2002). 2-aminoethoxydiphenyl borate (2-APB) is a reliable blocker of store-operated Ca^{2+} entry but an inconsistent inhibitor of $InsP_3$-induced Ca^{2+} release. FASEB J 16: 1145–1150.

Borisova L, Wray S, Burdyga T (2009). How structure, Ca signals and cellular communications underlie function in precapillary vessels. Circ Res 105: 803–810.

Bradley KN, Flynn ER, Muir TC, McCarron JG (2002). Ca^{2+} regulation in guinea-pig colonic smooth muscle: the role of the Na^+-Ca^{2+} exchanger and the sarcoplasmic reticulum. J Physiol 538: 465–482.

Bradley KN, Craig JW, Muir TC, McCarron JG (2004). The sarcoplasmic reticulum and sarcolemma together form a passive Ca^{2+} trap in colonic smooth muscle. Cell Calcium 36: 29–41.

Burdyga TV, Wray S (1999). The effect of cyclopiazonic acid on excitation-contraction coupling in guinea-pig ureteric smooth muscle: role of the sarcoplasmic reticulum. J Physiol 517: 855–865.

Burnstock G (2007). Physiology and pathophysiology of purinergic neurotransmission. Physiol Rev 87: 659–797.

Coussin F, Macrez N, Morel JL, Mironneau J (2000). Requirement of ryanodine receptor subtypes 1 and 2 for Ca^{2+}-induced Ca^{2+} release in vascular myocytes. J Biol Chem 275: 9596–9603.

Cupples WA, Braam B (2007). Assessment of renal autoregulation. Am J Physiol 292: F1105–F1123.

Davis MJ, Hill MA (1999). Signaling mechanisms underlying the vascular myogenic response. Physiol Rev 79: 387–423.

DiBona GF (2004). The sympathetic nervous system and hypertension: recent developments. Hypertension 43: 147–150.

Egan TM, Samways DS, Li Z (2006). Biophysics of P2X receptors. Pflugers Arch 452: 501–512.

Fabiato A, Fabiato F (1975). Contractions induced by a calcium-triggered release of calcium from the sarcoplasmic reticulum of single skinned cardiac cells. J Physiol 249: 469–495.

Feng JJ, Arendshorst WJ (1997). Calcium signaling mechanisms in renal vascular responses to vasopressin in genetic hypertension. Hypertension 30: 1223–1231.

Fill M, Copello JA (2002). Ryanodine receptor calcium release channels. Physiol Rev 82: 893–922.

Fisher SK, Domask LM, Roland RM (1989). Muscarinic receptor regulation of cytoplasmic Ca^{2+} concentrations in human SK-N-SH neuroblastoma cells: Ca^{2+} requirements for phospholipase C activation. Mol Pharmacol 35: 195–204.

Fleischmann BK, Wang YX, Pring M, Kotlikoff MI (1996). Voltage-dependent calcium currents and cytosolic calcium in equine airway myocytes. J Physiol 492: 347–358.

Foskett JK, White C, Cheung KH, Mak DO (2007). Inositol trisphosphate receptor Ca^{2+} release channels. Physiol Rev 87: 593–658.

George CH, Lai FA (2007). Developing new anti-arrhythmics: clues from the molecular basis of cardiac ryanodine receptor (RyR2) Ca^{2+}-release channel dysfunction. Curr Pharm Des 13: 3195–3211.

Gordienko DV, Bolton TB (2002). Crosstalk between ryanodine receptors and IP_3 receptors as a factor shaping spontaneous Ca^{2+}-release events in rabbit portal vein myocytes. J Physiol 542: 743–762.

Gordienko DV, Zholos AV (2004). Regulation of muscarinic cationic current in myocytes from guinea-pig ileum by intracellular Ca^{2+} release: a central role of inositol 1,4,5-trisphosphate receptors. Cell Calcium 36: 367–386.

Gordienko DV, Clausen C, Goligorsky MS (1994). Ionic currents and endothelin signaling in smooth muscle cells from rat renal resistance arteries. Am J Physiol 266: F325–F341.

Gordienko DV, Zholos AV, Bolton TB (1999). Membrane ion channels as physiological targets for local Ca^{2+} signalling. J Microsc 196: 305–316.

Gordienko DV, Greenwood IA, Bolton TB (2001). Direct visualization of sarcoplasmic reticulum regions discharging Ca^{2+} sparks in vascular myocytes. Cell Calcium 29: 13–28.

Gordienko DV, Harhun MI, Kustov MV, Pucovský V, Bolton TB (2008). Sub-plasmalemmal $[Ca^{2+}]_i$ upstroke in myocytes of the guinea-pig small intestine evoked by muscarinic stimulation: IP_3R-mediated Ca^{2+} release induced by voltage-gated Ca^{2+} entry. Cell Calcium 43: 122–141.

Guan Z, Osmond DA, Inscho EW (2007a). P2X receptors as regulators of the renal microvasculature. Trends Pharmacol Sci 28: 646–652.

Guan Z, Osmond DA, Inscho EW (2007b). Purinoceptors in the kidney. Exp Biol Med 232: 715–726.

Harhun MI, Szewczyk K, Laux H, Prestwich SA, Gordienko DV, Moss RF *et al.* (2009). Interstitial cells from rat middle cerebral artery belong to smooth muscle cell type. J Cell Mol Med 13: 4532–4539.

Harhun MI, Povstyan OV, Gordienko DV (2010). Purinoreceptor-mediated current in myocytes from renal resistance arteries. Br J Pharmacol 160: 987–997.

Hashitani H, Brading AF (2003). Ionic basis for the regulation of spontaneous excitation in detrusor smooth muscle cells of the guinea-pig urinary bladder. Br J Pharmacol 140: 159–169.

Hashitani H, Yanai Y, Kohri K, Suzuki H (2006). Heterogeneous CPA sensitivity of spontaneous excitation in smooth muscle of the rabbit urethra. Br J Pharmacol 148: 340–349.

Horowitz LF, Hirdes W, Suh BC, Hilgemann DW, Mackie K, Hille B (2005). Phospholipase C in living cells: activation, inhibition, Ca^{2+} requirement, and regulation of M current. J Gen Physiol 126: 243–262.

Hotta S, Yamamura H, Ohya S, Imaizumi Y (2007). Methyl-beta-cyclodextrin prevents Ca^{2+}-induced Ca^{2+} release in smooth muscle cells of mouse urinary bladder. J Pharmacol Sci 103: 121–126.

Inscho EW, Cook AK, Imig JD, Vial C, Evans RJ (2003). Physiological role for P2X1 receptors in renal microvascular autoregulatory behaviour. J Clin Invest 112: 1895–1905.

Isenberg G, Han S (1994). Gradation of Ca^{2+}-induced Ca^{2+} release by voltage-clamp pulse duration in potentiated guinea-pig ventricular myocytes. J Physiol 480: 423–438.

Iversen BM, Arendshorst WJ (1999). Exaggerated Ca^{2+} signaling in preglomerular arteriolar smooth muscle cells of genetically hypertensive rats. Am J Physiol 276: F260–F270.

Janiak R, Wilson SM, Montague S, Hume JR (2001). Heterogeneity of calcium stores and elementary release events in canine pulmonary arterial smooth muscle cells. Am J Physiol 280: C22–C33.

Ji G, Feldman M, Doran R, Zipfel W, Kotlikoff MI (2006). Ca^{2+}-induced Ca^{2+} release through localized Ca^{2+} uncaging in smooth muscle. J Gen Physiol 127: 225–235.

Kamishima T, McCarron JG (1996). Depolarization-evoked increases in cytosolic calcium concentration in isolated smooth muscle cells in rat portal vein. J Physiol 492: 61–74.

Kamishima T, McCarron JG (1997). Regulation of cytosolic Ca^{2+} concentration by Ca^{2+} stores in single smooth muscle cells from rat cerebral arteries. J Physiol 501: 497–508.

Kockskämper J, Zima AV, Roderick HL, Pieske B, Blatter LA, Bootman MD (2008). Emerging roles of inositol 1,4,5-trisphosphate signaling in cardiac myocytes. J Mol Cell Cardiol 45: 128–147.

Kohda M, Komori S, Unno T, Ohashi H (1997). Characterization of action potential-triggered $[Ca^{2+}]_i$ transients in single smooth muscle cells of guinea-pig ileum. Br J Pharmacol 122: 477–486.

Kotlikoff MI (2003). Calcium-induced calcium release in smooth muscle: the case for loose coupling. Prog Biophys Mol Biol 83: 171–191.

Lamb GD (2002). Excitation-contraction coupling and fatigue mechanisms in skeletal muscle: studies with mechanically skinned fibres. J Muscle Res Cell Motil 23: 81–91.

Lamont C, Wier WG (2004). Different roles of ryanodine receptors and inositol (1,4,5)-trisphosphate receptors in adrenergically stimulated contractions of small arteries. Am J Physiol 287: 617–625.

Laporte R, Hui A, Laher I (2004). Pharmacological modulation of sarcoplasmic reticulum function in smooth muscle. Pharmacol Rev 56: 439–513.

McCarron JG, Craig JW, Bradley KN, Muir TC (2002). Agonist-induced phasic and tonic responses in smooth muscle are mediated by $InsP_3$. J Cell Sci 115: 2207–2218.

McCarron JG, Chalmers S, Bradley KN, MacMillan D, Muir TC (2006). Ca^{2+} microdomains in smooth muscle. Cell Calcium 40: 461–493.

Mackrill JJ, Challiss RAJ, O'Connell DA, Lai FA, Nahorski SR (1997). Differential expression and regulation of ryanodine receptor and *myo*-inositol 1,4,5-trisphosphate receptor Ca^{2+} release channels in mammalian tissues and cell lines. Biochem J 327: 251–258.

MacMillan D, Chalmers S, Muir TC, McCarron JG (2005). IP_3-mediated Ca^{2+} increases do not involve the ryanodine receptor, but ryanodine receptor antagonists reduce IP_3-mediated Ca^{2+} increases in guinea-pig colonic smooth muscle. J Physiol 569: 533–544.

Malpas SC, Leonard BL (2000). Neural regulation of renal blood flow: a re-examination. Clin Exp Pharmacol Physiol 27: 956–964.

Moore ED, Voigt T, Kobayashi YM, Isenberg G, Fay FS, Gallitelli MF *et al.* (2004). Organization of Ca^{2+} release units in excitable smooth muscle of the guinea-pig urinary bladder. Biophys J 87: 1836–1847.

Morimura K, Ohi Y, Yamamura H, Ohya S, Muraki K, Imaizumi Y (2006). Two-step Ca^{2+} intracellular release underlies excitation-contraction coupling in mouse urinary bladder myocytes. Am J Physiol 290: C388–C403.

Navar LG (2005). The role of the kidneys in hypertension. J Clin Hypertens 7: 542–549.

Nishiyama A, Majid DS, Taher KA, Miyatake A, Navar LG (2000). Relation between renal interstitial ATP concentrations and autoregulation-mediated changes in renal vascular resistance. Circ Res 86: 656–662.

North RA (2002). Molecular physiology of P2X receptors. Physiol Rev 82: 1013–1067.

Ohi Y, Yamamura H, Nagano N, Ohya S, Muraki K, Watanabe M *et al.* (2001). Local Ca^{2+} transients and distribution of BK channels and ryanodine receptors in smooth muscle cells of guinea-pig vas deferens and urinary bladder. J Physiol 534: 313–326.

Peng Z, Dang A, Arendshorst WJ (2007). Increased expression and activity of phospholipase C in renal arterioles of young spontaneously hypertensive rats. Am J Hypertens 20: 38–43.

Poburko D, Fameli N, Kuo KH, van Breemen C (2008). Ca^{2+} signaling in smooth muscle: TRPC6, NCX and LNats in nanodomains. Channels 2: 10–12.

Povstyan OV, Harhun MI, Gordienko DV (2009). Electrical events and mechanisms of $[Ca^{2+}]_i$ mobilisation induced by P2X receptor stimulation in rat renal resistance artery myocytes. Proc Physiol Soc 15: PC18.

Powis G, Seewald MJ, Gratas C, Melder D, Riebow J, Modest EJ (1992). Selective inhibition of phosphatidylinositol phospholipase C by cytotoxic ether lipid analogues. Cancer Res 52: 2835–2840.

Prestwich SA, Bolton TB (1991). Measurement of picomole amounts of any inositol phosphate isomer separable by h.p.l.c. by means of a bioluminescence assay. Biochem J 274: 663–672.

Rahman T, Taylor CW (2009). Dynamic regulation of IP_3 receptor clustering and activity by IP_3. Channels 3: 226–232.

Rainbow RD, Macmillan D, McCarron JG (2009). The sarcoplasmic reticulum Ca^{2+} store arrangement in vascular smooth muscle. Cell Calcium 46: 313–322.

Sakai T, Terada K, Kitamura K, Kuriyama H (1988). Ryanodine inhibits the Ca-dependent K current after depletion of Ca stored in smooth muscle cells of the rabbit ileal longitudinal muscle. Br J Pharmacol 95: 1089–1100.

Shmigol A, Eisner DA, Wray S (1998). Properties of voltage-activated [Ca^{2+}] transients in single smooth muscle cells isolated from pregnant rat uterus. J Physiol 511: 803–811.

Smith RJ, Sam LM, Justen JM, Bundy GL, Bala GA, Bleasdale JE (1990). Receptor-coupled signal transduction in human polymorphonuclear neutrophils: effects of a novel inhibitor of phospholipase C-dependent processes on cell responsiveness. J Pharmacol Exp Ther 253: 688–697.

Somlyo AV, Somlyo AP (1968). Electromechanical and pharmacomechanical coupling in vascular smooth muscle. J Pharm Exp Ther 159: 129–145.

Surprenant A, North RA (2009). Signaling at purinergic P2X receptors. Annu Rev Physiol 71: 333–359.

Sutko JL, Airey JA, Welch W, Ruest L (1997). The pharmacology of ryanodine and related compounds. Pharmacol Rev 49: 53–98.

Suzuki M, Muraki K, Imaizumi Y, Watanabe M (1992). Cyclopiazonic acid, an inhibitor of the sarcoplasmic reticulum Ca^{2+}-pump, reduces Ca^{2+}-dependent K^+ currents in guinea-pig smooth muscle cells. Br J Pharmacol 107: 134–140.

Taylor CW, Traynor D (1995). Calcium and inositol trisphosphate receptors. J Mem Biol 145: 109–118.

Vagnes OB, Hansen FH, Feng JJ, Iversen BM, Arendshorst WJ (2005). Enhanced Ca^{2+} response to AVP in preglomerular vessels from rats with genetic hypertension during different hydration states. Am J Physiol 288: F1249–F1256.

Walsh MP (1994). Regulation of vascular smooth muscle tone. Can J Physiol Pharmacol 72: 919–936.

Wang SQ, Wei C, Zhao G, Brochet DX, Shen J, Song LS *et al*. (2004). Imaging microdomain Ca^{2+} in muscle cells. Circ Res 95: 798–806.

von der Weid PY, Rahman M, Imtiaz MS, van Helden DF (2008). Spontaneous transient depolarizations in lymphatic vessels of the guinea pig mesentery: pharmacology and implication for spontaneous contractility. Am J Physiol 290: H813–H822.

White C, McGeown JG (2002). Carbachol triggers RyR-dependent Ca^{2+} release via activation of IP_3 receptors in isolated rat gastric myocytes. J Physiol 542: 725–733.

White C, McGeown JG (2003). Inositol 1,4,5-trisphosphate receptors modulate Ca^{2+} sparks and Ca^{2+} store content in vas deferens myocytes. Am J Physiol 285: C195–C204.

White SM, Imig JD, Kim TT, Hauschild BC, Inscho EW (2001). Calcium signaling pathways utilized by P2X receptors in freshly isolated preglomerular MVSMC. Am J Physiol 280: F1054–F1061.

Wibo M, Godfraind T (1994). Comparative localization of inositol 1,4,5-trisphosphate and ryanodine receptors in intestinal smooth muscle: an analytical subfractionation study. Biochem J 297: 415–423.

Wier WG, Balke CW (1999). Ca^{2+} release mechanisms, Ca^{2+} sparks, and local control of excitation-contraction coupling in normal heart muscle. Circ Res 85: 770–776.

Wier WG, Morgan K (2003). α_1-adrenergic signalling mechanisms in contraction of resistance arteries. Rev Physiol Biochem Pharmacol 150: 91–139.

Wier WG, Zang WJ, Lamont C, Raina H (2009). Sympathetic neurogenic Ca^{2+} signalling in rat arteries: ATP, noradrenaline and neuropeptide Y. Exp Physiol 94: 31–37.

Wray S, Burdyga T (2010). Sarcoplasmic reticulum function in smooth muscle. Physiol Rev 90: 113–178.

Zhang WM, Yip KP, Lin MJ, Shimoda LA, Li WH, Sham JS (2003). ET-1 activates Ca^{2+} sparks in PASMC: local Ca^{2+} signaling between inositol trisphosphate and ryanodine receptors. Am J Physiol 285: L680–L690.

Zhao X, Cook AK, Field M, Edwards B, Zhang S, Zhang Z *et al*. (2005). Impaired Ca^{2+} signaling attenuates P2X receptor-mediated vasoconstriction of afferent arterioles in angiotensin II hypertension. Hypertension 46: 562–568.

ZhuGe R, Sims SM, Tuft RA, Fogarty KE, Walsh JV Jr (1998). Ca^{2+} sparks activate K^+ and Cl^- channels, resulting in spontaneous transient currents in guinea-pig tracheal myocytes. J Physiol 512: 711–718.

ZhuGe R, Bao R, Fogarty KE, Lifshitz LM (2010). Ca^{2+} sparks act as potent regulators of excitation-contraction coupling in airway smooth muscle. J Biol Chem 285: 2203–2210.

Zizzo MG, Mulè F, Serio R (2006). Mechanisms underlying hyperpolarization evoked by P2Y receptor activation in mouse distal colon. Eur J Pharmacol 544: 174–180.